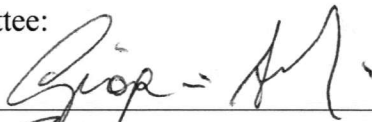


ESTIMATION OF THE POPULATION SIZES OF NEURONAL TYPES OF THE
HIPPOCAMPOME KNOWLEDGE BASE IN THE DENTATE GYRUS

by

Sean Mackesey
A Thesis
Submitted to the
Graduate Faculty
of
George Mason University
in Partial Fulfillment of
The Requirements for the Degree
of
Master of Science
Bioinformatics and Computational Biology

Committee:



Dr. Giorgio Ascoli, Thesis Director



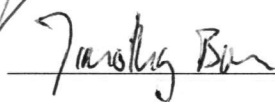
Dr. Iosif Vaisman, Committee Member



Dr. Padmanabhan Seshaiyer, Committee Member



Dr. James D. Willett, Director, School of Systems Biology



Dr. Timothy L. Born, Associate Dean for Student and Academic Affairs, College of Science



Dr. Peggy Agouris, Interim Dean, College of Science

Date: 08/01/2013

Fall Semester 2013
George Mason University
Fairfax, VA

Estimation of the Population Sizes of Neuronal Types of the Hippocampome Knowledge
Base in the Dentate Gyrus

A thesis submitted in partial fulfillment of the requirements for the degree of
Master of Science at George Mason University

By

Sean Mackesey
Bachelor of Arts
Northwestern University, 2008

Director: Dr. Giorgio Ascoli, Professor
Department of Bioinformatics and Computational Biology

Fall 2013
George Mason University
Fairfax, VA

Copyright © 2013 by Sean Mackesey
All Rights Reserved

Dedication

Dedicated to Somnus, the God of Sleep

Acknowledgments

I would like to thank the following people who made this possible ... Christopher Rees first and foremost, for being mind-bogglingly helpful and supportive during the writing process; Diek Wheeler, Charise White, Alexander Komendantov, and David Hamilton for all of their hard work on the Hippocampome; and my advisor, Giorgio Ascoli, for welcoming me into neuroinformatics and teaching me so much.

Table of Contents

	Page
List of Figures	x
Abstract	xii
1 Introduction	1
1.1 Motivation	1
1.2 Problem Statement	1
1.3 Thesis Overview	2
2 The Hippocampome	3
2.1 Overview of the Hippocampome	3
2.2 Neuronal Classification	3
3 The Dentate Gyrus	7
3.1 Anatomy	7
3.2 Neuron Types	9
3.2.1 Mossy and Quadrilaminar Mossy	10
3.2.2 Hilar Granule	11
3.2.3 Hilar Interneurons	11
3.2.4 Granule	13
3.2.5 SG Interneurons	13
3.2.6 SM Neurons	14
3.3 Regional Counts and Distributions of Neurons	14
4 History of Neuronal Counts in the Dentate Gyrus	18
4.1 Past Efforts to Indirectly Determine Neuron Numbers	18
4.2 Patton and McNaughton 1995	19
4.2.1 Granule Cells	19
4.2.2 Basket Cells	19
4.2.3 Axo-Axonic Cells	20
4.2.4 Gabaergic Peptidergic Polymorphic Cells and Mossy Cells	20
4.3 Dyhrfeld-Johnsen and Soltesz 2007	21
4.3.1 HIPP and HICAP	21
4.3.2 Interneuron-Specific	21

4.3.3	MOPP	21
4.4	Evaluation of Past Efforts in the Context of the Hippocampome	22
4.4.1	Equating Basket Cells with most GABAergic neurons in the Hilus	23
4.4.2	Ratio of Axo-Axonic to Granule Cells	23
4.4.3	Equating HIPP Cells with SOM+ Cells in the Hilus	23
4.4.4	Equating HICAP Cells with nNOS+/CR-/NPY-/SOM- Neurons in the Hilus	24
4.4.5	Estimating the Number of MOPP cells based on an even distribution of GABAergic neurons in the molecular layer	25
4.4.6	Interneuron-Specific cells are the CR+ Aspiny Cells of the Hilus	25
5	Data Mining	26
5.1	Data Pipeline	26
5.2	Literature Search	26
5.2.1	Discovery	28
5.2.2	Evaluation	29
5.3	Annotation	30
5.3.1	All Data Types	31
5.3.2	Morphological Ratios	31
5.3.3	Stereological Neuron Counts, Densities, and Ratios	32
5.3.4	Volumes	33
6	Input Data	34
6.1	Overview of Input Data	34
6.2	Morphological Ratios	34
6.3	Stereological Counts	39
6.4	Assumptions	39
7	Optimization	40
7.1	Optimization Overview	40
7.2	Equation Generation	40
7.2.1	Ratios	40
7.2.2	Stereological Counts	42
7.2.3	Markers	42
7.3	Analysis of Constraints	45
7.3.1	Constrained and Unconstrained Parameters	45
8	Results and Discussion	48
8.1	Description of Results	48

8.2	Interpretation of Results	50
8.3	Reliability of Constraints	50
8.4	Future Directions	51
A	Neuron Types of the Dentate Gyrus	53
B	List of Constraints	59
B.1	Assumption	59
B.1.1	Ratio of GABAergic Neurons in SMO:SMi is 2:1	59
B.2	Morphological Ratio	60
B.2.1	Armstrong C, Szabadics J, Tamas G, Soltesz I. Neurogliaform cells in the molecular layer of the dentate gyrus as feed-forward gamma-aminobutyric acidergic modulators of entorhinal-hippocampal interplay. <i>J Comp Neurol</i> 2011.	60
B.2.2	Buckmaster PS, Strowbridge BW, Kunkel DD, Schmiede DL, Schwartzkroin PA. Mossy cell axonal projections to the dentate gyrus molecular layer in the rat hippocampal slice. <i>Hippocampus</i> 1992.	61
B.2.3	Buckmaster PS. Mossy cell dendritic structure quantified and compared with other hippocampal neurons labeled in rats in vivo. <i>Epilepsia</i> 2012.	62
B.2.4	Ceranik K, Bender R, Geiger JR, Monyer H, Jonas P, Frotscher M, Lubke J. A novel type of GABAergic interneuron connecting the input and the output regions of the hippocampus. <i>J Neurosci</i> 1997.	63
B.2.5	Han ZS. Electrophysiological and morphological differentiation of chandelier and basket cells in the rat hippocampal formation: a study combining intracellular recording and intracellular staining with biocytin. <i>Neurosci Res</i> 1994.	64
B.2.6	Lubke J, Frotscher M, Spruston N. Specialized electrophysiological properties of anatomically identified neurons in the hilar region of the rat fascia dentata. <i>J Neurophysiol</i> 1998.	66
B.2.7	Mott DD, Turner DA, Okazaki MM, Lewis DV. Interneurons of the dentate-hilus border of the rat dentate gyrus: morphological and electrophysiological heterogeneity. <i>J Neurosci</i> 1997.	67
B.2.8	Williams PA, Larimer P, Gao Y, Strowbridge BW. Semilunar granule cells: glutamatergic neurons in the rat dentate gyrus with axon collaterals in the inner molecular layer. <i>J Neurosci</i> 2007.	69
B.3	Stereology	70

B.3.1	Buckmaster PS, Jongen-Relo AL. Highly specific neuron loss preserves lateral inhibitory circuits in the dentate gyrus of kainate-induced epileptic rats. J Neurosci 1999.	70
B.3.2	Jiao Y, Nadler JV. Stereological analysis of GluR2-immunoreactive hilar neurons in the pilocarpine model of temporal lobe epilepsy: correlation of cell loss with mossy fiber sprouting. Exp Neurol 2007. . .	74
B.3.3	Rapp PR, Gallagher M. Preserved neuron number in the hippocampus of aged rats with spatial learning deficits. Proc Natl Acad Sci U S A 1996.	76
B.3.4	Woodson W, Nitecka L, Ben-Ari Y. Organization of the GABAergic system in the rat hippocampal formation: a quantitative immunocytochemical study. J Comp Neurol 1989.	77
C	Boundary Conditions	80
C.1	Granule Cells	80
C.2	Hilar Granule Cells	81
C.3	Mossy and Quadrilaminar Mossy	81
C.4	Semilunar Granule Cells	81
C.5	Interneurons	81
D	Annotation Format	83
D.1	Annotation Motivation	83
D.2	Content	83
D.3	Syntax	84
D.3.1	Design Principles	84
D.3.2	Base Format	85
D.3.3	Data Fields by Annotation File Type	85
E	Annotation Samples	89
E.1	Morphological Ratio File	89
E.2	Stereology File	94
E.3	Type File	95
F	Literature Search Records	98
F.1	Publications Completely Mined for Citations of Interest	98
F.2	Abstracts Evaluated for Morphological Ratios	98
F.3	Full Text Evaluated for Morphological Ratios	101
F.4	Abstracts Evaluated for Stereology	111
F.5	Full Text Evaluated for Stereology	112

Bibliography 118

List of Figures

Figure	Page
3.1 Hippocampal Formation (Allen Brain Explorer)	7
3.2 Hippocampus in Cross Section (van Strien et al 2010)	8
3.3 Counts and Distributions by Layer	17
5.1 Data Pipeline	27
5.2 Literature Search Summary	29
5.3 Criteria of Relevance	30
7.1 Soma Matrix	41
7.2 Equations from a Ratio	41
7.3 Known Marker Expression and Estimates of Layer-Specific Marker-Positive Counts	43
7.4 Row-Reduced Echelon Form	46
7.5 Well-Constrained Parameters	47
8.1 Optimization Results	48
8.2 Comparison of Results with Past Efforts	49
A.1 Granule (+)2201p (Lubke & Spruston 1998)	53
A.2 Semilunar Granule (+)2311p (Williams et al 2010)	53
A.3 Quad MC (+)2323 (Scharfman 2012)	54
A.4 Hilar Granule (+)2203p (Marti-Subirana et al 1986)	54
A.5 Mossy (+)0103 (Buckmaster et al 1992)	54
A.6 Total Molecular (-)3303 (Bartos et al 2010)	54
A.7 MOLAX (-)3302 (Soriano & Frotscher 1993)	55
A.8 Outer Molecular (-)3222 (Mott et al 1997)	55
A.9 Neurogliaform (-)3000p (Armstrong et al 2011)	55
A.10 MOPP (-)3000 (soma SMO) (Armstrong et al 2011)	55
A.11 MOPP (-)3000 (soma SMi) (Han et al 1993)	55
A.12 Aspiny Hilar (-)2333 (Lubke & Spruston 1998)	56
A.13 HICAP (-)2322 (soma SG) (Mott et al 1997)	56

A.14 HICAP (-)2322 (soma H) (Han et al 1993)	56
A.15 Axo-Axonic (-)2233 (Soriano & Frotscher 1989)	56
A.16 Basket-PV (-)2232 (Bartos et al 2001)	57
A.17 Basket-CCK (-)2232 (soma SMi) (Hajos et al 1996)	57
A.18 Basket-CCK (-)2232 (soma SG) (Hajos et al 1996)	57
A.19 Hilar proj (-)1333p (Lubke & Spruston 1998)	57
A.20 HIPPP (-)1002 (soma SG) (Han et al 1993)	58
A.21 Non-Ivy / NGF (-)0331 (Markwardt et al 2011)	58
C.1 Boundary Conditions	82

Abstract

ESTIMATION OF THE POPULATION SIZES OF NEURONAL TYPES OF THE HIPPOCAMPOME KNOWLEDGE BASE IN THE DENTATE GYRUS

Sean Mackesey, MS

George Mason University, 2013

Thesis Director: Dr. Giorgio Ascoli

The Hippocampome is a new knowledge base of neuron types in the rodent hippocampus that aims to compile and collate the mass of published information regarding the cellular constituency of this structure. The foundation of the Hippocampome is a set of morphologically distinct neuron types, defined by the presence of axons and dendrites within specific anatomical compartments of the hippocampal formation. Primary aims of the Hippocampome include the creation of a standard classification scheme for hippocampal neurons and the establishment of a central repository for knowledge about the properties of these neurons. The present project attempts to derive the population size estimates for the 18 Hippocampome neuron types with somata in the dentate gyrus, one of the hippocampal formation's major constituents. Data from morphological and stereological studies was taken from the literature and represented as a system of equations constraining the population sizes of the dentate gyrus neuron types. A simulated annealing algorithm was used to optimize the system and thereby provide estimates for the population sizes. It is hoped that this work serve as a pilot for future, larger scale attempts to derive population estimates for all Hippocampome types.

Chapter 1: Introduction

1.1 Motivation

The hippocampus has long been a region of interest to computational modelers. It plays a critical role in memory and epilepsy, and has been the beneficiary of more than 100 years of research. Many attempts have been made to build hippocampus models that are scaled down in both the total number of neurons and neuron types (Santhakumar et al 2005). Every year, more computational power becomes available to researchers and reduces the technical limits that necessitate these simplifications. At the same time, the collected knowledge of hippocampal neuron types is continually expanding. The Hippocampome aims to catalog this growing list of types and the data required to generate the parameters to model them. Plainly, the number of instantiated neurons of each type will play a major role in the network dynamics of such a model (Patton & McNaughton 1995). Such numbers should be informed by an accurate estimate of the true distribution of neurons across the existing types. Thus, the compilation of accurate type population sizes is a central piece of the Hippocampome.

1.2 Problem Statement

The population sizes of the different neuronal types of the dentate gyrus are mostly unknown. This thesis aims to accomplish two goals:

1. Compile existing population size data in the dentate gyrus and determine its representation in terms of Hippocampome cell types
2. Analyze the compiled data and establish what may be inferred from it and which unknowns would, if resolved, provide the greatest utility in inference

1.3 Thesis Overview

This thesis provides an estimate of the population size of each of the Hippocampome neuronal types in the dentate gyrus. The estimates have been generated by a simulated annealing algorithm, used to optimize a system of equations generated by representing empirical data in terms of the Hippocampome ontology. These data have been taken from a variety of experiments that were published in years ranging from 1981 to 2012. The data are of three sorts: integer ratios of morphologically-defined neuronal populations, stereologically derived estimates of the population sizes of chemically-defined populations, and stereologically-derived estimates of ratios between chemically-defined populations. The interpretation of the data was informed by past efforts at inferring the counts of dentate gyrus neuron types (Patton & McNaughton 2005, Dyhrfeld-Johnsen et al 2007). A discussion of dentate gyrus anatomy and neuron types, the history of the problem of finding neuron counts for these types, and the employed methods of literature search and annotation are presented in addition to results and discussion.

Chapter 2: The Hippocampome

2.1 Overview of the Hippocampome

The Hippocampome is a knowledge base of the neuron types of the rodent hippocampus. It has been built up through the mining of the rich hippocampus literature for descriptions of neurons. In any literature mining project, decisions must be made as to what information is important enough to extract. For the Hippocampome, these decisions have been guided by the requirements of a large-scale circuit model of the hippocampus. Such a model requires connectivity, population size, and functional data. Molecular marker expression data have also been collected, in part for their potential utility in inferring population sizes.

Currently, the Hippocampome hosts 122 different neuronal types. These types are a mixture of classically recognized (e.g. basket) and more recently discovered, unnamed neurons. Each type has associated with it evidence (figures and quotes) extracted from the literature concerning its morphological, molecular marker expression, and electrophysiological properties.

The Hippocampome went public in late 2012 and is available at: <http://hippocampome.org>

2.2 Neuronal Classification

The Hippocampome aims to establish a standard way of classifying neurons. This effort takes place in the context of a varied history of neuronal classification. In the past, neurons were frequently classified by the location and shape of their somata (Amaral 1978; Ribak & Seress 1983), as these were the neuronal properties most readily apparent from bulk dye tissue stains. The introduction of biocytin as an intracellular labeller by Horikawa (1988)

made possible many more complete reconstructions of single neurons than were previously obtainable. This led to a boom in studies that classified neurons according to their arborization pattern (e.g. Han et al 1993, Mott et al 1997) and allowed the axo-dendritic morphologies of relatively large numbers of neurons to be characterized in conjunction with electrophysiological recordings of those neurons. Immunolabeling and more recently in situ hybridization have enabled the classification of neurons based on their expression of specific proteins and mRNA, respectively. Either may be used to identify proteins uniquely associated with a particular neurotransmitter.

Thus, there are five primary axes for the classification of neurons: soma location and morphology, axo-dendritic morphology, marker expression, primary neurotransmitter, and electrophysiological function. As there is no standardized hierarchy, different researchers choose to emphasize different properties. To further complicate matters, in many cases, the lack of accepted naming and classification conventions result in the same name being given to neurons with different properties by different researchers.

This is relevant because the Hippocampome, and the present thesis in particular, relies upon the mapping of descriptions taken from the literature into the particular classification scheme undergirding the Hippocampome. This scheme is founded on the premise that, besides the primary neurotransmitter, axo-dendritic morphology is the most important property of a neuron. This is because the locations of a neuron's axons and dendrites determine its potential connectivity with other neurons and thus the potential structure of the network. The axo-dendritic morphology is defined within the confines of a regional parcellation scheme that identifies six major subregions of the hippocampal complex: the dentate gyrus (DG), cornu ammonis (CA3, CA2, CA1), the subiculum (SUB), and the entorhinal cortex (EC). Each of these regions is split into 3-6 layers, for a total of 26 anatomical compartments.

Hippocampome neuron types, with a few exceptions, have a unique axo-dendritic pattern within this scheme. This may be thought of as a 26-dimensional quaternary vector where each element represents the presence of axons, dendrites, both, or neither in the

corresponding compartment. The presence or absence of axons, dendrites in these compartments are hereafter referred to as “formal properties”. Differences in soma location among neurons with the same axo-dendritic pattern are not sufficient to split a type. However, the compartmental somata locations of neurons with a given axo-dendritic pattern have been recorded, so soma location is also a formal property. Formal properties may be contrasted with properties such as the density of arborization, origin of the axon, or shape of the soma. These “informal” properties are not captured in the Hippocampome but are frequently described by authors.

In order to extract Hippocampome-compatible morphological information from the literature, references are evaluated with respect to the set of formal properties. Consequently, the neurons of interest must be described with sufficient clarity that their axons or dendrites can be definitively said to be present within one parcel and not another. This can be problematic when the authors of the study of interest were classifying their neurons according to other priorities. While some morphological information is typically given, it is frequently vague and requires interpretation.

The uncertainty inherent in a human interpreter ‘binarizing’ such a complex structure as a neuron, described in vague language, has necessitated the creation of objective rules for the assignments of morphological properties. All of these rules, and particularly those pertaining to author word choice, are very imperfect. Words such as “some”, “most”, and “sparse” are ultimately subjective, yet these words can make the difference between the formal establishment of a Hippocampome type and the potential passing over of a passage in the literature. In the case of mining data relative to cell counts, they can affect the content of an equation derived from the passage. By applying conservative interpretations wherever possible, an effort has been made to minimize this sort of error.

Finally, it must be noted that the Hippocampome’s list of neuron types is not yet complete. It is hoped that in time, enough clear evidence will come to the fore to resolve most of the partial evidence that has accumulated for a type. In the meantime, however, the incompleteness is the source of some discrepancies within the literature. In the present

project, when a population of neurons encountered in the literature is not consistent with any Hippocampome type, it has been tagged for review but ignored for the purpose of calculating neuron counts. This is undoubtedly a source of error.

Chapter 3: The Dentate Gyrus

3.1 Anatomy

The dentate gyrus (DG) is one constituent of the hippocampal formation (Figure 3.1). It borders on the hippocampus proper (also known as “cornu ammonis” (CA) or “Ammon’s horn”) and the subiculum. The rat dentate gyrus, like the hippocampus proper, extends from a dorso-rostral pole located near the septum back to a ventro-caudal pole located next to the temporal lobe. Hence the two poles are sometimes referred to as septal and temporal, and the curved axis connecting them is termed the septotemporal axis. The overall shape is reminiscent of a banana. Because there are separate hippocampi in the left and right hemispheres, there are also two dentate gyri.

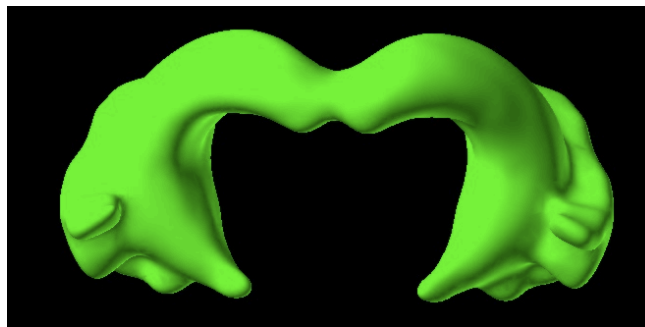


Figure 3.1: Hippocampal Formation (Allen Brain Explorer)

The DG has traditionally been split into three layers visible in cross-section in Figure 3.2: the stratum moleculare (SM), stratum granulosum (SG), and hilus (H), sometimes referred to as the polymorph layer. SG is far more densely packed with cell somata than either of

the other layers. Its primary constituents are the so-called “granule cells”, named for their small cell bodies. Due to their large numbers, they are the “principal cells” of the DG, and SG is referred to as the “principal cell layer”. The granule cells residing in SG receive inputs from the entorhinal cortex. These inputs are carried by the fibers of the perforant path, a tract initiating in the EC, passing through the subiculum, and terminating in SM of the DG on granule cell dendrites. In turn, the axons of granule cells, or “mossy fibers”, extend through the hilus towards the CA3 area, where they synapse on the dendrites of pyramidal cells. An additional distinction is sometimes made between the third of SM bordering SG and the other two thirds, which are referred to as the inner and outer strata moleculare (SMi and SMo), respectively (Amaral & Lavenex 2007).

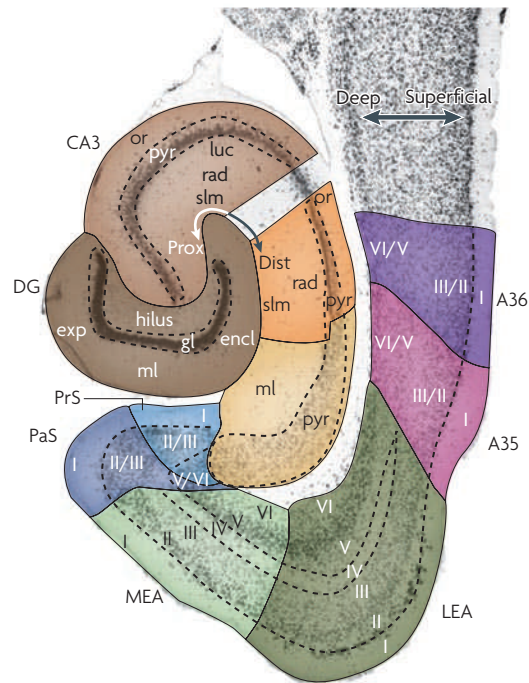


Figure 3.2: Hippocampus in Cross Section (van Strien et al 2010)

3.2 Neuron Types

Traditionally, the neurons of the dentate gyrus have been split into two broad categories: principal (granule) cells and interneurons. The term “interneuron” has traditionally meant a neuron whose neurites are confined to a local circuit. These stand in contrast to projection neurons. In the hippocampus, the vast majority of such neurons are GABAergic, which has led to the use of “interneuron” to refer to hippocampal GABAergic neurons generally. This is a somewhat controversial use of the term, however, as several studies have demonstrated the existence of dentate GABAergic neurons that project to CA3 and the subiculum (Ceranik et al 1997; Lubke et al 1998). Nonetheless, Freund and Buzsaki (1996), in a seminal review of hippocampal interneurons, advocate equating the term with “GABAergic non-principal cell”. That is the sense in which it will be used here.

While there is a greater variety of GABAergic than glutamatergic neurons in the dentate gyrus, the population of glutamatergic neurons is much higher. The primary reason for this is that granule cells are excitatory (Amaral & Lavenex 2007), and granule cells are clearly the most populous neuron type (this is obvious from visual inspection of a Nissl-stained slice). However, normal granule cells are not the only glutamatergic neuron present. Amaral (1978) coined the term “mossy cell” to describe a type of neuron with its somata in the hilus that received efferents from granule cell mossy fibers. For some time there was debate as to the glutamatergic status of mossy cells (Scharfman & Myers 2012), but Soriano and Frotscher (1994) provided evidence that mossy cells were glutamatergic by showing that they were glutamate-immunoreactive. While the majority of mossy cells have their dendrites confined to the hilus, there is a significant subpopulation that sends a small number of dendrites to the molecular layer (Buckmaster 2012; Buckmaster et al 1992). In the Hippocampome, these have been called “quadrilaminar mossy cells” (Quad MC). There are also a small number of ectopic granule cells found in the hilus (Marti-Subirana et al 1986).

The 18 known neuron types of the dentate gyrus are summarized below by layer, with reference to obtaining their counts. An image of each neuron type can be found in Appendix

A.

3.2.1 Mossy and Quadrilaminar Mossy

Mossy cells are one of the most famous neuron types in the hilus. They are also relatively populous (Buckmaster et al 1999) and electrophysiologically distinct from interneurons (Scharfman & Myers 2012). This combination of history, abundance, and distinctiveness has made mossy neurons one of the better quantitatively characterized types in the dentate gyrus.

One approach to counting mossy cells is to use hilar glutamatergic neurons as a proxy. This approach is justified by the fact that mossy cells are clearly the dominant glutamatergic type in the hilus (Scharfman & Myers 2012). There are different approaches to approximating the glutamatergic count. Buckmaster and Jongen-Relo (1999) used the optical fractionator to estimate both the total number and the number of GAD-positive neurons in the hilus. The difference yielded an estimate of the glutamatergic count. Jiao and Nadler (2007) counted neurons immunoreactive for the GluR2 subunit of the AMPA receptor. Sloviter et al (2001) found that coexpression of GluR2 and GABA occurred in less than 1% of all hilar neurons, suggesting that very few GABAergic neurons are GluR2-immunoreactive and that a count of mGluR2-IR neurons is therefore a good estimate of the number of glutamatergic.

The type of neuron that most authors call ‘mossy’ is actually representative of two different Hippocampome types. The Hippocampome distinguishes between mossy cells that extend dendrites through the granule layer into the deep molecular layer, and those that do not. The former type are called “quadrilaminar”, in reference to the presence of dendrites in all four Hippocampome-recognized layers of the dentate gyrus. The literature does not contain any direct efforts to ascertain the ratio of these two types of mossy cell, but an estimate may be derived from two different studies. Buckmaster (2012) sampled 12 mossy cells for a detailed analysis of dendritic structure and found 3 of them to extend dendrites to the molecular layer. An earlier study conducted by Buckmaster et al (1992)

focused on the axonal projections of mossy cells and found 6 of 41 with dendrites in the molecular layer.

3.2.2 Hilar Granule

McCloskey et al (2006) and Jiao and Nadler (2007) both estimated the number of hilar ectopic granule cells and arrived at answers that differed by a factor of 10 (~ 1000 for McCloskey; ~ 100 for Jiao). The discrepancy is likely due to different methods used in the two studies. McCloskey counted neurons expressing the nuclear protein PROX-1. PROX-1 is known to be expressed in normal granule cells (Pleasure et al 2000) and has also been used for the detection of displaced granule cells in CA3 (Szabadics et al 2010). While most interneurons do not express PROX-1, it is unknown whether there is a small population of hilar interneurons that do. It is also possible that some neurons express a protein that cross-reacts with the PROX-1 antibody. Jiao and Nadler (2007) counted GluR2-immunoreactive neurons. Both estimates make assumptions about the marker expression status of largely unexplored hilar interneurons. The reliability of Jiao's estimate is dependent on the GluR2-negative status of hilar interneurons, whereas McCloskey's depends on the PROX-1 negative status of the same neurons. Since there is better evidence for the former (cf Section 3.2.1; Sloviter et al 2001), Jiao's estimate appears more reliable.

3.2.3 Hilar Interneurons

The hilus contains a diverse array of interneurons and remains relatively unexplored. Because of the diversity of neuron types here, it is difficult to determine the count of any one type. However, attempts have been made to estimate counts of HIPP and HICAP, the two most well-known interneuron types in this region, by equating them to certain classes of neurochemically defined neurons (cf Chapter 4). Both types were named by Han et al (1993). These neurons differ primarily by their layer of arborization. HIPP cells target the outer molecular layer, whereas HICAP target the inner molecular layer. In addition, HICAP cells have dendrites that extend through all layers of the dentate gyrus where HIPP

dendrites are confined to the hilus.

HIPP and HICAP neurons are possibly the most populous, and are perhaps most famous merely because they were some of the first hilar interneurons to have their axonal arborizations visualized. It seems likely that there are actually far more types present in this region, though perhaps in low numbers. Lubke and Spruston (1998) identified several other varieties of interneurons, which are described as “very variable in their dendritic morphology”. Only a subset of them were presented as figures, however, so the full extent of the variability could not be gauged. The Hippocampome formally recognizes two types taken from this paper: Hilar Projecting and Aspiny Hilar.

Furthermore, the Hippocampome contains records of several other varieties of hilar interneurons, but they are backed by insufficient evidence for formal inclusion in the Hippocampome. Most of these ‘frozen’ types come from a study by Hajos and Freund (1996), who looked at the highly morphologically variable population of VIP+ neurons in the dentate gyrus. They describe a number of interneuron-specific cells, but the reconstructions are few in number and the population so variable that there is only a single example of several axo-dendritic patterns, which is insufficient for inclusion in the Hippocampome. Soltesz et al (1993) describe and provide a single figure of a mossy cell with significant dendritic arborization in CA3c. This type has not been described elsewhere. Finally, Gulyas et al (1996), in a study of calretinin-immunoreactive neurons, described another interneuron-specific type located in the hilus.

The fact that the evidence for all but one of the frozen types (the Soltesz mossy cell variant) comes from studies targeting specific neurochemically-defined populations indicates that these populations are not well-characterized. It is likely that future studies of VIP and CR-positive dentate neurons will provide sufficient evidence to make at least some of the frozen types into formal Hippocampome classes. Because so little is currently known of them, however, they are not included in the present analysis.

3.2.4 Granule

The only glutamatergic neurons of SG are the granule cells. Their number may be estimated by combining a stereological estimate of the total number of neurons in SG (Rapp & Gallagher 1996; West et al 1991) with the percentage of SG neurons that are glutamatergic, known to be approximately 98 (Woodson et al 1989; Babb et al 1988).

3.2.5 SG Interneurons

The stratum granulosum is home to a variety of interneurons clustered primarily along its two borders with the hilus and molecular layer (Freund & Buzsaki 1996). These most famously include the basket cell, a neuron found throughout the CA regions as well as the dentate gyrus. Dentate basket cells have a dense arborization in the granule layer and extend dendrites throughout all layers of the dentate gyrus. Basket cells have historically been subclassified into various groups depending on the location and size of their somata (Ribak & Seress 1983). This distinction is not considered to be significant in the Hippocampome, since all of these types share the same axo-dendritic arborization. More recently, they have been divided into PV and CCK-positive populations (Freund & Buzsaki 1996).

The second most well-known SG interneuron is the axo-axonic cell (Han et al 1993; Freund & Buzsaki 1996). These neurons have distinctive vertically-oriented axons within SG that contact the axon initial segments of granule cells.

Studies of the SG/H border by Mott et al (1997, 1999), Scharfman (1995), and Soriano and Frotscher (1993) have revealed a variety of other interneurons that innervate the molecular layer. Unlike the interneurons of the hilus, which tend to innervate specifically the inner or outer molecular layer, these neurons send diffuse axons throughout its entire extent.

As with hilar interneurons, the diversity of interneuron types in this region makes the estimation of any one type's count difficult. Nonetheless, attempts have been made to estimate the ratios of basket and axo-axonic cells to granule cells by using their estimated

ratio (cf Chapter 4; Patton & McNaughton 1995; Dyhrfeld-Johnsen et al 2007).

3.2.6 SM Neurons

The molecular layer is very sparsely populated (Woodson et al 1989). The best known neuron type in this region is the MOPP cell, named by Han et al (1993). MOPP cells have been observed with somata in both the inner and outer molecular layers (Hajos et al 1996), with both axons and dendrites confined to the outer molecular layer. Studies by Ceranik et al (1997) and Armstrong et al (2011) identified an additional neuron type, called Neurogliaform, that is similar to MOPP but also projects to the subiculum. Both of these studies provide ratios of MOPP to Neurogliaform cells. Patton & McNaughton (1995) and Dyhrfeld-Johnsen et al (2007) have estimated the counts of MOPP cells by assuming that they were the only neurons present in the molecular layer and assuming an even distribution of somata.

In the inner molecular layer, Williams et al (2007) and Larimer and Strowbridge (2010) have identified a population of glutamatergic neurons known as Semilunar Granule Cells. These are the only known glutamatergic neurons in SM.

Basket cells have been observed near the SG/SMi border region that stain positive for CCK and VIP (Hajos et al 1996).

Ceranik et al (1997) has observed a population of neurons projecting to the CA3 region that is not consistent with any Hippocampome type. This is because the Ceranik paper has not yet been formally processed for type extraction. This type may later be included in the Hippocampome.

3.3 Regional Counts and Distributions of Neurons

The regional totals of neurons in the stratum granulosum and hilus of the dentate gyrus have been explored by many investigators. The majority of these studies make no distinction between neuron types (Boss et al 1985; Gaarskjaer 1978; Hosseini-Sharifabad & Nyengaard

2007; Miki et al 2005; West & Andersen 1980; West et al 1991; Rapp & Gallagher 1996). Stains such as NeuN or cresyl-violet are used to visualize the cell bodies of neurons, which are counted in systematically sampled sections. A neuron count is then derived using any of several different methods.

The total number of GABAergic neurons in the dentate gyrus has been estimated by Buckmaster et al (1999), who found approximately 36,000. The distribution of these neurons across the three major layers of the dentate gyrus was also estimated, yielding a ratio of 47:26:27 in the hilus, granule, and molecular layers respectively.

Babb et al (1988) and Woodson et al (1989) both investigated the distribution of GABA across the whole hippocampus and the percentage of neurons within each layer that were GABAergic. Babb found that 2, 26, and 23 percent of neurons were GAD+ in SG, H, and SM respectively. Woodson found 2 percent in SG and 42 percent in the molecular layer. Woodson divided what is usually called the hilus into two different zones: the “polymorph layer” and the “hilar region”. The polymorph layer was defined as “the subgranular zone boarding the hilus . . . [that] contains many GABA-Li neuronal somata.” The hilar region contained only 18% GABAergic somata, while the polymorph layer showed significant differences along the axis running from the suprapyramidal to infrapyramidal blade, averaging approximately 40%. The discrepancy between estimates of the GABAergic percentage in the molecular layer bears note. Because the molecular layer is so sparsely populated (Woodson et al 1989) relative to the granule layer, measurements of the percentage of GABAergic neurons are extremely sensitive to where the border is drawn. Neither of these studies make the location of this border very clear.

The estimated counts for the stratum granulosum span a wide range: 600,000 to 2,000,000 (Patton & McNaughton 2005). These discrepancies are likely due to either differences between strains and ages of rats or methodological errors. Boss et al (1985) found that the number of granule cells varies significantly during the first year of life in Wistar but not Sprague-Dawley rats. A more likely source of the greatest discrepancies is error due to

biased stereological methods. Many studies published in the 1980s and 1990s used methods of estimation, such as the Abercrombie correction, that rely on assumptions about the orientation of cell somata and that are vulnerable to double-counting error (West 1999). Most recent stereological work has corrected these methodological flaws and uses unbiased methods, such as the optical fractionator. West et al (1991) and Rapp and Gallagher (1996) both obtained estimates of approximately 1.2 million neurons in SG using the optical fractionator. This is the number accepted in the present study.

The hilus has also been a subject of stereological investigations. Buckmaster et al (1999) and West et al (1991) counted the total numbers of neurons in the hilus, finding approximately 46,000 total neurons. The difference of the total and GABAergic counts has been interpreted as the number of mossy cells, as they are the major glutamatergic cell type in the hilus. Jiao and Nadler (2007) counted the numbers of glutamatergic neurons using a marker for GluR2.

No quantitative literature was found concerning the distribution of either all or GABAergic somata between the inner and outer molecular layers.

■ Computed ■ Literature

	Count			Distribution		
	Total	GABA	GLUT	Total	GABA	GLUT
DG	1.20E+06	3.59E+04	1.20E+06	1	1	1
DG:SMo	2.30E+04	9.60E+03	0	0.018	0.27	0
DG:SMi			1.30E+04			0
DG:SG	1.20E+06	9.30E+03	1.20E+06	0.95	0.26	0.99
DG:H	4.67E+04	1.68E+04	2.93E+04	0.036	0.47	0.01

Figure 3.3: Counts and Distributions by Layer

Chapter 4: History of Neuronal Counts in the Dentate Gyrus

4.1 Past Efforts to Indirectly Determine Neuron Numbers

As with the present study, the impetus behind past attempts to estimate neuronal counts in the dentate gyrus has been the necessity of counts for computational models. The first major attempt to summarize and synthesize the available data was made by Patton and McNaughton (1995). This paper reviews the cell number data available at the time and attempts to estimate the counts for selected types. Patton estimated the counts of 5 kinds of neurons: 1,000,000 granule cells, 30,000 mossy cells, 10,000 basket cells, 1,000 axo-axonic cells, and 15,000 gabaergic peptidergic polymorphic cells. “GABAergic peptidergic polymorphic” cell should be regarded as a synonym of “hilar interneuron”. More types were recognized by Patton than had their counts estimated; MOPP and diverse VIP+ neurons were excluded due to lack of data.

More recently, researchers at the University of California, Irvine, also seeking counts for a computational model, have attempted to build on Patton’s work. A series of modeling studies and reviews use an identical set of neuron types and nearly identical estimates of their counts (Dyhrfeld-Johnsen et al 2007; Morgan et al 2007; Santhakumar 2008; Morgan & Soltesz 2010). The studies share a common logic (detailed below). It is articulated in most detail in Dyhrfeld-Johnsen (2007). Counts were estimated for eight types. Four of these types correspond directly with Patton’s: granule, basket, axo-axonic, and mossy cells. For granule and basket cells, both the estimated count and logic are the same as used by Patton. For axo-axonic cells, the logic is similar, but where Patton estimates 1,000 neurons, Dyhrfeld-Johnsen estimates 2,000. For mossy cells, the logic is different but the estimated count is the same, 30,000.

The four additional estimates provided by Dyhrfeld-Johnsen are for 4,000 MOPP, 12,000

HIPP, 3,000 HICAP, and 3,000 IS (interneuron-specific) cells. HIPP, HICAP, and IS cells in combination map to Patton and McNaughton's GABAergic peptidergic polymorphic group. Where Patton estimated 15,000 neurons, Dyhrfeld-Johnsen estimates 18,000.

Both the methods of reasoning and results are similar in these two studies, despite their 12-year separation. Patton and McNaughton stress the uncertainty in their estimates of basket and axo-axonic counts, yet Dyhrfeld-Johnsen et al use essentially the same estimates and justification. This is indicative of the slow progress in this area.

The major difference between the two lies in the chemically-defined population data used by Dyhrfeld-Johnsen that was not available at the time of Patton's estimates. These data consist of counts of SOM+ (somatostatin), CR+ (calretinin), and nNOS+ (neuronal nitric oxide synthase) neurons, as well as data on their coexpression. A correlation between expression of these markers and morphology was exploited, and counts of immunopositive cells were used as proxies for the counts of morphologically-defined HIPP, HICAP, and IS neurons. Similar reasoning was recently used by Bezaire & Soltesz (2013) to approximate the counts of many types found in CA1.

The logic and estimates used in the Patton & McNaughton and Dyhrfeld-Johnsen and Soltesz studies are presented by type below, followed by an examination of this logic in the context of the Hippocampome.

4.2 Patton and McNaughton 1995

4.2.1 Granule Cells

Citing West et al (1991), a study of granule cell numbers using the optical fractionator, Patton adopts an estimate of 1,000,000 granule cells.

4.2.2 Basket Cells

Two lines of reasoning are employed to arrive at a basket cell estimate.

Citing Celio et al (1990), which found 4,000 PV+ neurons in the DG, and Ribak et al

(1990), which found that 32-38% of all basket cell terminals onto granule cells are PV+, Patton assumes that all or most PV+ neurons are basket cells, Patton adopts an estimate of 10,000 basket cells.

Secondly, the study references the Babb et al (1988) and Woodson et al (1989) findings that roughly 2% of neurons in SG are GABAergic. Assuming that most of these neurons are basket cells, Patton again arrives at an estimate of 10,000 basket cells.

It should be noted that Patton cites Seress and Pokorny (1981) as well, who counted basket cells and found a range of 2,900 to 4,000. However, for unstated reasons, the higher value of 10,000 is chosen for the model.

4.2.3 Axo-Axonic Cells

Patton's estimate of axo-axonic cells derives from Li et al (1992), which found a ratio of between 150 and 600 pyramidal cells to every axo-axonic cell in CA1. In a personal communication with Peter Somogyi, Somogyi stated that he believed the number of granule cells contacted by a single dentate axo-axonic cell is larger than the number of pyramidal cells contacted by a CA1 axo-axonic cell, which led to the final estimate of 1,000 axo-axonic cells in the dentate gyrus.

4.2.4 Gabaergic Peptidergic Polymorphic Cells and Mossy Cells

Citing the stereology of West et al (1991), Patton estimates that there are a total of 50,000 neurons in the hilus. Employing the Rapp et al (1988) finding of 30% SOM+ neurons in the hilus, and assuming that all SOM+ neurons are GABAergic, Patton estimates there to be 15,000 gabaergic peptidergic polymorphic cells. Citing a personal communication with Sloviter, who estimated 10% of all hilar neurons to be subgranular zone basket cells, 5,000 neurons are estimated to be basket cells. The remaining 30,000 neurons in the hilus are assumed to be mossy cells.

4.3 Dyhrfjeld-Johnsen and Soltesz 2007

4.3.1 HIPP and HICAP

Citing the Buckmaster et al (1999) finding of 12,000 somatostatin-positive neurons in the hilus, Dyhrfjeld-Johnsen estimated 12,000 HIPP neurons, under the assumption that the set of SOM+ neurons was identical with the set of HIPP neurons.

Adopting a similar strategy of equating a neuron type to a unique molecular profile, Dyhrfjeld-Johnsen obtained an estimate of HICAP cells. The group cited Nomura et al (1997), which found 7,000 nNOS+ neurons in the hilus, of which roughly half were negative for CR, NPY, and SOM, Dyhrfjeld-Johnsen estimated 3,000 HICAP cells, under the assumption that the set of nNOS+/CR-/NPY-/SOM- neurons was identical with HICAP neurons.

4.3.2 Interneuron-Specific

In obtaining an estimate for interneuron specific cells, Dyhrfjeld-Johnsen assumed that the set of aspiny CR+ neurons was identical with IS cells. Citing a Nomura et al (1997a,b) finding of 6,500 CR+ neurons in the hilus, and assuming that less than half of them are aspiny, Dyhrfjeld-Johnsen posited 3,000 IS cells.

4.3.3 MOPP

Citing the Buckmaster et al (1999) estimate of roughly 10,000 molecular layer GABAergic neurons, and assuming an even distribution of these cells across the molecular layer (without evidence), Dyhrfjeld-Johnsen estimated that there were 4,000 GABAergic neurons in the outer molecular layer. All of these were assumed to be MOPP cells.

4.4 Evaluation of Past Efforts in the Context of the Hippocampome

The sources of both of the above studies' estimates can be split into two categories: (1) stereology-derived estimates and logical reasoning with ratios of neuron types or and (2) assumed correspondences between morphologically-defined types and neurochemically-defined types.

Similar stereological findings to those used for the total count of granule cells and both the total count and GABAergic count of neurons in the hilus have been incorporated into the present study. However, the value of 1,200,000 (West et al 1991; Rapp & Gallagher 1996) was used for the total number of neurons in SG rather than the 1,000,000 used by Patton and Dyhrfeld-Johnsen. Both Rapp and West found a count of 1.2 million neurons using the same modern stereological method, the optical fractionator. Both Patton and Dyhrfeld-Johnsen cite West, and it is unknown why they rounded the estimate of 1,200,000 down to 1,000,000.

The steps of inference used to determine the other counts are examined below with respect to the Hippocampome's unique context. This context is distinct in several important ways from that of the above efforts. The Hippocampome distinguishes between many more dentate gyrus interneuron types than either of the above studies. What either group calls a 'basket cell' may correspond to more than one Hippocampome type. Furthermore, the increased number of types means that greater precision is required in the estimates, since these types necessarily have smaller populations than the broader types described above.

The assumptions made by the Patton and Dyhrfeld-Johnsen studies are now taken in turn and evaluated critically with the benefit of additional time passed and the knowledge compiled in the Hippocampome. In each case, a binary judgment is made regarding the usability of the assumption as a constraint in this thesis project.

4.4.1 Equating Basket Cells with most GABAergic neurons in the Hilus

Both Patton and Dyhrfeld-Johnsen obtained a rough estimate of the GABAergic count in SG from Babb et al (1988) and Woodson et al (1989). “Many” of these neurons were assumed basket cells. No evidence is presented to support this claim; furthermore, the Hippocampome has 9 different interneurons in the granule layer, where both Patton and Dyhrfeld-Johnsen distinguish only two (basket and axo-axonic). Thus, many of what might be called “basket” cells by either group may be classified differently in the Hippocampome. For this reason, the logic employed in the earlier studies was not used here.

4.4.2 Ratio of Axo-Axonic to Granule Cells

Both Patton and Dyhrfeld-Johnsen cite the work of Li et al (1992), who found a broad range for the ratio of axo-axonic to CA1 pyramidal neurons. They choose different seemingly arbitrary values at the upper end of this range. Because this range is so broad, the selection of different points within it for use as a constraint would have very different effects on the ratio of Hippocampome axo-axonic to other Hippocampome SG interneurons. Thus this logic was not used.

4.4.3 Equating HIPP Cells with SOM+ Cells in the Hilus

Dyhrfeld-Johnsen asserts that HIPP cells are equivalent to SOM+ neurons in the hilus. If Dyhrfeld-Johnsen is correct and ‘HIPP’ here corresponds to a superset of Hippocampome types, then this equivalence is usable as a constraint. Two papers are cited: Katona (1999) and Freund and Buzsaki (1996).

Katona conducted a study of SOM+ neurons in the hilus. Three neurons were reconstructed and all had the characteristics of HIPP cells: dendrites confined to the hilus, and dense axonal arborization in the outer molecular layer. However, one of these neurons retained axon collaterals in the hilus. Furthermore, several other neurons are described that had an axon that traveled to the outer molecular layer and then back to the hilus. These characteristics (cell body in H, dendrites only in H, axons in both H and SMO) are not

consistent with any neuron type in the Hippocampome. However, it is possible that these axons did not have sufficient density to pass the Hippocampome threshold. As it stands, there is only one Hippocampome type consistent with the description of most of the cells, and that is the HIPP cell.

Freund and Buzsaki (1996) are also cited by Dyhrfeld-Johnsen. Their position on this issue is stated clearly: “The correlation of morphology and neuro- chemical character for this cell type is perhaps the most straightforward of all such attempts; thus, “SOM cells” and “HIPP cells” in the dentate gyrus can be considered as synonymous.” HIPP cells are earlier described in a way consistent with the Hippocampome description, though it is mentioned that some have minor varicosities in the inner molecular layer.

Based on these citations, it can be asserted with some reservation that SOM+ cells may be equated with HIPP cells in the present state of the Hippocampome. However, this was not incorporated as a constraint in the present study due to software limitations at the time of analysis on the incorporation of molecular marker data.

4.4.4 Equating HICAP Cells with nNOS+/CR-/NPY-/SOM- Neurons in the Hilus

Dyhrfeld-Johnsen cites Nomura et al (1997a,b) to obtain a count of nNOS+/CR-/NPY-/SOM- neurons in the hilus. This is assumed to be equal to the number of HICAP cells, presumably because HIPP and IS neurons, the only other hilar interneurons under consideration, are positive for SOM and CR, respectively, and NPY is known to colocalize significantly with both CR and SOM (Kohler 1982). Because the Hippocampome has several additional types in the hilus with unknown expression of these markers, this assumption is not appropriate for the present study.

4.4.5 Estimating the Number of MOPP cells based on an even distribution of GABAergic neurons in the molecular layer

Dyhrfeld-Johnsen cite Buckmaster and Jongen-Relo (1999) for an estimated count of 10000 molecular layer interneurons. The GABAergic neurons of the molecular layer are assumed to be evenly distributed, implying a count of approximately 4000 MOPP neurons in the inner molecular layer. No evidence is presented for the even distribution of GAD+ neurons in the molecular layer. An examination of Woodson et al (1989) and Babb et al (1988), the two primary sources on the distribution of GABAergic somata in DG, is indeterminate. Thus the assumption of even distribution was not used.

4.4.6 Interneuron-Specific cells are the CR+ Aspiny Cells of the Hilus

Dyhrfeld-Johnsen estimate the number of interneuron-specific neurons in the hilus with aspiny CR+ neurons. The Hippocampome currently does not recognize any interneuron-specific cells in the hilus. While some types with frozen status do potentially correspond, because there are no corresponding Hippocampome types, this logic was excluded from the current project.

Chapter 5: Data Mining

5.1 Data Pipeline

All data used in this project underwent multiple stages of processing to convert the raw literature into information that was ready for consumption by the optimization algorithm. The pipeline is currently implemented in a partially manual, partially automated form. The automated parts of the pipeline use software in the Ruby language written by the author. It is hoped that more of the process can be automated as the Hippocampome becomes larger in scope.

The pipeline has three broad stages– literature search, annotation, and formatting for optimization.

5.2 Literature Search

A project such as this one should be comprehensive in its search for data. While a full survey of the literature was not achieved (a large number of articles remain queued for review), the literature was systematically searched and annotated. The records of all examined articles and the resulting annotations are stored in a database, which should allow future researchers to resume the search without duplication of effort. The content of this database is summarized in Appendix F.

Publications were evaluated for relevance to two kinds of data:

- morphological ratios obtained from studies that reconstructed small populations of neurons (305 abstracts mined; 84 full-text mined)
- stereologically-obtained count, density, and volume estimates (38 abstracts mined; 62 full-text mined)

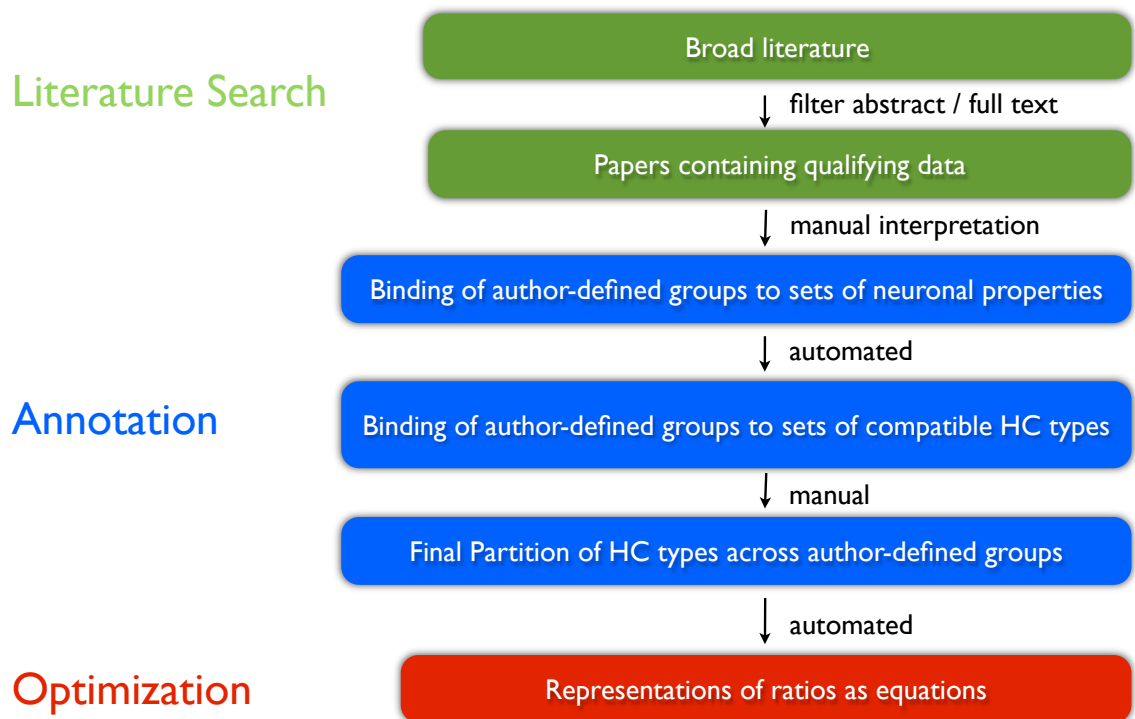


Figure 5.1: Data Pipeline

5.2.1 Discovery

Publications were discovered and added to the mining queue by three methods: (1) targeted PubMed queries (2) following citations from a selected set of reviews as well as any citations of interest encountered in other articles (3) taking publications included in the Hippocampome that were used as evidence for a dentate gyrus neuron types

Targeted PubMed Queries

PubMed searches were conducted with experimental software designed by this author to streamline annotation of abstracts. The system uses the PubMed API and filters out result publications that have already been annotated or queued for annotation, allowing the user to run a large number of similar queries without needing to sift through duplicates. This allows comprehensive search of a domain to be achieved efficiently. The software was used primarily to search for morphological ratios of dentate gyrus neurons. To learn more about this system, which is presently undergoing rapid development, contact the author.

Publications Mined for Citations of Interest

A select set of papers were completely mined for cited publications of interest. A publication of interest was any that was cited in the context of stereology, neuron counts, or comparative morphology of all or a chemically-defined subset of dentate gyrus interneurons. The set of publications fully mined for such citations was restricted to reviews and modeling papers, though citations of interest from other publications were sometimes followed as well. See Appendix F for a list of these publications.

Hippocampome Publications

The Hippocampome contains a list of publications used as evidence for the definition of neuronal types (cf Chapter 2). The dentate gyrus types that are the subject of this project all have at least one such publication. The full text of each article was evaluated for relevance.

5.2.2 Evaluation

Publications were evaluated in two stages: abstract and full-text review. The abstract was first evaluated for relevance. If the abstract was deemed relevant, then the full text of the article was subsequently evaluated. Publications with relevant full-text were selected for data extraction. In some cases, the relevance of abstracts of publications obtained from either the Hippocampome or a citation of interest could reasonably be assumed, and the abstract evaluation stage skipped. The criteria used to determine relevance are presented in Figure 5.3.

While there is significant overlap among the publications evaluated for morphological ratios and stereological count, density, and volume estimates, not every publication was formally evaluated for both kinds of data. Such partial evaluation of a publication was typical when the publication was obtained by a targeted literature search. A summary of the numbers of articles evaluated for each kind of data is presented in Figure 5.2. “Extracted” in this table refers to the number of articles that have been fully processed and annotated. These articles’ data is immediately ready for consumption by the scheme presented in Chapter 7.

	Morphology		Stereology	
	Positive	Reviewed	Positive	Reviewed
Abstract	120	305	13	38
Full Text	24	84	8	62
Extractions	13		7	

Figure 5.2: Literature Search Summary

Criteria of Relevance

Most of the criteria of relevance for both abstract and full-text evaluation were different for each data type. These criteria are summarized in Figure 5.3. While an effort was made to adhere to and expand this set of criteria to cover all cases, some cases nonetheless required subjective judgment.

	Both	Morphological Ratios	Stereological Estimates
Abstract	species was rat or mouse; region was dentate gyrus; subjects were postnatal	Golgi staining, whole-cell recording, or biocytin/Neurobiotin filling of neurons	mentioned volume of a dentate gyrus subregion or distribution, density, or total count of all, GABAergic/GLUTamatergic, or particular-marker-positive neurons in a dentate gyrus subregion
Full Text		contained a partition of reconstructed neurons into well-defined groups, with average size of a group ≥ 4	contained a numerical estimate of volume, or the density or count of all, GABAergic/GLUTamatergic, or marker-positive neurons in a dentate gyrus subregion

Figure 5.3: Criteria of Relevance

5.3 Annotation

Publications that passed the literature screening stage were processed differently depending on the data type contained by the publication. In all cases, the data was extracted in a specific format that compromises between principles of human-readability, machine-readability, and modularity. The details of the formats and processing software for each data type can be found in Appendix D. Below, the content of the annotations is described for each data type.

5.3.1 All Data Types

All publications that were mined for any data type had information about the species, strain, age, weight, and sex of the subjects extracted.

5.3.2 Morphological Ratios

Publications containing morphological ratios were first scanned for passages containing descriptions of author-defined neuronal populations. Such populations were identified whenever the authors contrasted one set of neurons with one or more others and assigned a number of neurons counted for each set. Sometimes, the author explicitly named a population. In these cases, the name used by the author was associated with the passages. When the author did not explicitly name the population, a name was determined for it according to the properties that distinguished it from other populations.

After the identification and grouping of passages under population names, each passage was associated with a list of properties that could reasonably be judged to apply to *all* neurons in the population. When the passage associated a property with the population using words such as “mostly”, “frequently”, or “often”, this property was not included. Properties apparent only in figures referenced by the passages were also excluded. The region from which the neurons were sampled was also recorded.

The lists included both formal and informal Hippocampome properties. As described in Section 2.2, the only formal morphological properties were the location of axons, dendrites, and somata in one of the 26 Hippocampome parcels. The recording of formal properties was desirable but usually insufficient to capture the full extent of the authors’ description. Thus, other properties describing characteristics such as arborization density and soma shape were recorded when necessary. Once a name for an informal property was assigned, the same name was used in other annotations. The most frequently occurring of these properties are future candidates for formalization. These include axonal target (soma/dendrites/ axon initial segment), arborization density, and location of somata in a border region. Full property lists for all ratios included in the present study can be found in Appendix B.

After property extraction, software was used to query the Hippocampome database and generate a list of all active Hippocampome neuron types consistent with each population’s *formal* properties. Because the informal properties were not tracked by the Hippocampome, the list of formally compatible types had to be manually evaluated for consistency with the informal properties.

This manual evaluation was performed by checking the defining Hippocampome descriptions of each type for consistency with the informal properties of the population(s) with which that type was formally consistent. Frequently, some neuron types were formally consistent with more than one population, but exclusion based on this manual evaluation was sufficient to eliminate it from consistency with all but one population. An example may be found in Appendix B.2 under Han (1994), where Axo-Axonic cells were formally consistent with both the “chandelier” and “basket” group. This was because the property of targeting axon initial segments (a defining feature of axo-axonic cells) is informal; taking this property into account allows the assignment of Axo-Axonic to the “chandelier” group.

In other cases, a neuron type was determined to be inconsistent with all populations—this was the case when dealing with populations taken from laminar borders, which are not formally recognized by the Hippocampome, as well as populations selected according to electrophysiological criteria. An example may be found in Appendix B.2 under Buckmaster (1992), where all interneuronal types are dissociated from any group on the basis of electrophysiological informal properties. The reasoning employed for excluding neuron types from formally compatible populations was recorded in annotation files, described in Appendix D.

5.3.3 Stereological Neuron Counts, Densities, and Ratios

Publications containing stereologically derived counts, densities, and ratios were scanned for tables and passages containing these quantities. As with the neurons described in publications containing morphological ratios, the populations with which a number was associated were annotated with lists of properties. This process was straightforward, because the

described populations were defined purely by molecular marker expression (inferred from immunocytochemical staining) and/or soma location. No attempt was made to distinguish between different strengths of marker expression. Software was used to query the Hippocampome database and determine a set of types consistent with the formal properties describing each population.

In some cases, informal marker expression properties were associated with a population. Because all marker-expression/soma-location properties with known information were formal, it was not possible to perform a manual evaluation of types against the informal properties. However, these properties may become useful when data associating them with Hippocampome types is incorporated into the Hippocampome in the future.

5.3.4 Volumes

Publications containing volumes were scanned for numerical values. Frequently, these publications were the same ones containing stereological neuron counts or densities, as volume is often an input in the calculation needed to obtain estimated count or density from the raw data.

Chapter 6: Input Data

6.1 Overview of Input Data

A subset of extracted data was used to generate the system of equations that was optimized. This data included 8 morphological ratios, a direct count of hilar granule cells, a total GABAergic count across all of the DG, the laminar distribution of GABAergic neurons across SM, SG, and H, a total count of neurons in SG, a total count of neurons in H, a count of GABAergic neurons in H, a count of glutamatergic neurons in H, and percentages of neurons in SG and SM that are GABAergic. These quantities are not all independent of one another, and when there was no good reason to choose one over another, both were included. These data are presented in Appendix B.

Data from studies of molecular markers other than GAD and GluR2 were not used, because the expression data associating these markers with Hippocampome types was too incomplete. See Section 7.2.2 for more on this issue.

6.2 Morphological Ratios

7 different morphological ratios were extracted from the literature and used as constraints. A “ratio” here means separate counts of two or more distinct groups of neurons. The ratios presented below range from a minimum of 12 (Han et al 1993; Buckmaster 2012) to a maximum of 41 (Buckmaster et al 1992) total neurons sampled. Any ambiguities encountered in the mapping of author-defined groups to Hippocampome types is described.

Buckmaster et al 1992

41 neurons from H were reconstructed. These neurons were selected according to the distinct physiology of mossy cells, as this was the target of the authors' interest. Therefore, all GABAergic neurons have been excluded.

The mapping to Hippocampome types is straightforward. Two groups were delineated on the basis of the presence of dendrites in SM, a distinction which also serves as the primary factor separating the two Hippocampome mossy types, Mossy and Quad MC. Because of the age of the study, and the authors indication that the filling was often incomplete, the true number of neurons extending dendrites to SM may have been greater than the 6 they found.

Han et al 1994

A total of 12 interneurons were taken from the granule cell layer and the hilus. They were classified according to their dominant pattern of arborization into basket cells targeting somata in SG, chandelier cells targeting axon initial segments, and axo-dendritic (i.e. dendrite-targeting) cells innervating the molecular layer.

Since chandelier (axo-axonic) neurons are highly distinctive and there is a strong consensus as to their definition in the community, the sole chandelier cell was counted as axo-axonic.

The authors say that axons in the basket cell group were “mainly distributed evenly throughout the entire length of the principle cell layer”. Though they do not say that there were no axons in SM, the fact that they specified a separate group (axo-dendritic) neurons that projected to SM suggests that any basket cells with significant arborization in SM would be included in this group or singled out for mention. Therefore, non-ivy/NGF, hilar-projecting, and aspiny hilar neurons, all of which have significant projections to SM, are included in the axo-dendritic group.

Ceranik et al 1997

40 neurons were reconstructed from the outer molecular layer. They were classified according to their axonal arborization and with the exception of putative “displaced granule cells”, which stood out due to somata size. Some of the neurons were found to project to the subiculum.

The mapping to Hippocampome types is straightforward in this instance. The primary distinguishing factor between Neurogliaform (NGF) and MOPP neurons is the NGF projection to the SLM, which is the same distinction the authors used.

One group was found to project to CA1:SLM. There were no Hippocampome types matching either this group or the displaced granules. These groups were therefore excluded from the ratio.

Mott et al 1997

A total of 40 neurons on the border between the granule layer and the hilus were classified. Neurons were grouped primarily by the layer in which axonal arborization was densest. The groups were named “OML” (outer molecular layer), “IML” (inner molecular layer), “TML” (total molecular layer), and “GCL” (granule cell layer).

It is possible that some of the neurons classified by Mott as OML and IML might be classified in the Hippocampome as MOLAX or Total Molecular. This is because the axons of IML and OML neurons were said to exist “predominantly” in the SMi or SMO, respectively— it is not clear that all of these neurons lacked, by Hippocampome standards, axons in the other part of the molecular layer. Nonetheless, a judgment was made to assign MOLAX and Total Molecular neurons exclusively to the TML group for the present project.

Hilar projecting neurons, while formally consistent with several of Mott’s groups, were excluded from all groups for two reasons. First, projections to CA3 are a prominent feature of Hilar Projecting neurons, and no such projections are described by Mott and Lewis. Furthermore, it is unknown whether these neurons reside at the SG/H border. The only known figure of a Hilar Projecting neuron (Lubke et al 1998) shows a soma located deeper

within the hilus, and the authors state that “[these neurons] usually had somata in the deep hilus” (cf. “aspiny hilar interneurons with axonal projections to the outer molecular layer”, Lubke et al 1998).

Lubke et al 1998

A total of 17 non-mossy neurons throughout the hilus, including the SG/H border region, were classified. The criteria of morphological classification were spininess and the locations of axons and dendrites. Though mossy cells were also examined, they are excluded from this ratio because the total number of them is not given.

The authors distinguished between spiny and aspiny interneurons with a projection to the outer molecular layer, but the Hippocampome does not distinguish based on spines. Therefore these two author-defined groups were merged for the present purpose.

The authors point out that 1 of the 6 observed basket cells was projecting to the inner molecular layer. They provide a figure of this neuron but the quantity of arborization in SMi does not meet the Hippocampome threshold. Therefore this neuron was grouped with the other basket cells.

Zhang et al 2009

181 neurons from the SG/H border region were reconstructed. The subjects were a mix of rats with pilocarpine-induced status epilepticus and control rats. While the authors were looking for basket cells, they state that the only criteria for selecting a cell for recording was the size of the soma.

Because this data comes in part from epileptic animals, it was not used as a source of constraints and not fully processed. However, it is included here because it is still relevant to the status of neuron counts in the dentate gyrus.

Armstrong et al 2011

17 neurons were sampled from the outer molecular layer. The authors were searching for neurogliaform cells. Though they filled other neurons as part of their search, they do not describe the morphology of these neurons in any detail, nor do they offer a count. Therefore the only ratio that could be extracted was the one between two different types of subtypes of the neurons the authors sought. 11 of 17 of Armstrong's "Neurogliaform" neurons projected to SUB, and 6 did not. In the Hippocampome, only the projecting cells are called NGFCs. The others were likely MOPP cells.

Buckmaster 2012

12 neurons were reconstructed from H. Though the author does not describe the sampling method, it is stated that they are mossy cells. This is confirmed by the presence of thorny excrescences. Therefore all GABAergic neurons are excluded, as well as hilar granule cells (which also lack thorny excrescences).

The author distinguishes two groups of neurons on the basis of dendrites in SM. The groups correspond respectively with Hippocampome classes Mossy (no dendrite in SM) and Quad MC.

Discrepancies

There is a significant discrepancy between the results of Mott et al and Zhang et al. Both experiments sampled from the SG/H border zone, but they found vastly different ratios of neurons arborizing primarily in SG to other kinds of cells. Mott et al found only 4/40 neurons to arborize primarily SG, whereas Zhang et al found 153/181. While some of this discrepancy is likely due to the fact that some of Zhang's data came from an epilepsy model, this is unlikely to explain all of it. However, it is known that the vast majority of GABAergic neurons lost in the hilus in a kainate-induced model of epilepsy are SOM-positive (Buckmaster & Jongen-Relo 1999); and HIPP cells are known to be positive for SOM while basket are negative. Further experiments are needed to determine the true

ratios in this region.

6.3 Stereological Counts

The counts that were included as constraints were presented in Section 3.3. They are also included in the list of all constraints in Appendix B.

6.4 Assumptions

Based on examinations of line drawings by Woodson et al (1989), the distribution of GAD-positive neurons in the molecular layer was judged to be even. The number of neurons visible in these line drawings is quite small, however, and a detailed study is needed to approximate the true distribution. Such an analysis is possible with the use of StereoNavigator software and high-resolution images taken from <http://brainmaps.org>.

Chapter 7: Optimization

7.1 Optimization Overview

The data mined from the literature were used to estimate neuronal counts via a simulated annealing optimization algorithm implemented in the R language (Xiang et al). This required the representation of the data as equations in terms of a parameter scheme. Below is presented an explanation of the mapping from data to equations, an analysis of how constrained the system was following this mapping, and an interpretation of the meaning of these constraints.

7.2 Equation Generation

The equations constructed were composed entirely of constants (data from the literature) and parameters representing the layer-specific populations of Hippocampome types. The matrix in Figure 7.1 is a representation of the distribution of somata of dentate gyrus types. A red square at the intersection of a type row and a layer column represents the presence of the type's somata in that layer. A parameter can be assigned to each red square representing the size of this type population. Type totals can be recovered by summing across the parameters for a particular row.

7.2.1 Ratios

An n-way ratio was converted into n-1 equations via a simple algorithm. In the example shown in Figure 7.2 below, Mott et al (1997) noted 5 groups of cells within the dentate gyrus (Figure 7.2, first column) in the ratio of 4:8:6:11:11. To translate this information into

Neuron Type	DG				Occupied Squares
	S M o	S M i	S G	H	
Granule (+)2201p					23
Semilunar Granule (+)2311p					
Quad MC (+)2323					
Hilar Granule (+)2203p					
Mossy (+)0103					
Total Molecular (-)3303					
MOLAX (-)3302					
Outer Molecular (-)3222					
Neurogliaform (-)3000p					
MOPP (-)3000					
Aspiny Hilar (-)2333					
HICAP (-)2322					
Axo-Axonic (-)2233					
Basket-PV (-)2232					
Basket-CCK (-)2232					
Hilar proj (-)1333p					
HIPP (-)1002					
Non-Ivy / NGF (-)0331					

Figure 7.1: Soma Matrix

equations, the populations were first placed in an arbitrary sequence. Next, each author-defined group was mapped to Hippocampome types sharing properties associated with that population. Subsequently, the parameters representing the layer-specific populations of these Hippocampome types were collected. Finally, for each pair of adjacent groups in this sequence, an equation was generated equating the empirical ratio of these populations to the ratio of the parameter sums associated with each population.

Group Name	Mapped Types	Equation
4 GCL cells	Basket-PV Basket-CCK	$\frac{4}{8} = \frac{DG:SG:Basket-PV + DG:SG:Basket-CCK}{DG:SG:HICAP + DG:H:HICAP + DG:SG:Aspiny\ Hilar + DG:H:Aspiny\ Hilar + DG:SG:Non-Ivy / NGF}$
8 IML cells	HICAP Aspiny Hilar Non-Ivy / NGF	$\frac{8}{6} = \frac{DG:SG:HICAP + DG:H:HICAP + DG:SG:Aspiny\ Hilar + DG:H:Aspiny\ Hilar + DG:SG:Non-Ivy / NGF}{DG:SG:Outer\ Molecular + DG:SG:HIPP + DG:H:HIPP}$
6 OML cells	Outer Molecular HIPP	$\frac{6}{11} = \frac{DG:SG:Outer\ Molecular + DG:SG:HIPP + DG:H:HIPP}{DG:SG:Total\ Molecular}$
11 TML cells with axon in H	Total Molecular	$\frac{11}{11} = \frac{DG:SG:Total\ Molecular}{DG:SG:MOLAX}$
11 TML cells with no axon in H	MOLAX	

Figure 7.2: Equations from a Ratio

7.2.2 Stereological Counts

Equations were generated for counts by equating the empirical count value with a sum of parameters representing a partition of the type population. In equation (7.1), a count of GABAergic neurons in the hilus is set equal to the sum of hilar GABAergic populations.

$$\text{Count GABA}^+ \text{ in H} = \sum \text{GABA}^+ \text{ H populations} \quad (7.1)$$

$$16801 = \text{DG:H:HICAP} + \text{DG:H:HIPP} + \text{DG:H:Hilar proj} + \text{DG:H:Aspiny Hilar}$$

The process is straightforward when the given count is of either all neurons or GABAergic neurons. A neuron count may be expressed as an equation by setting the left side equal to the count and the right side equal to a sum of representative type populations.

7.2.3 Markers

Molecular markers such as parvalbumin, calretinin, and calbindin are a potential source of constraints. Immunohistochemical stains have been used to visualize the neurons expressing these markers, allowing stereological estimates of the size of marker-expressing populations. Given sufficient knowledge of the expression status of Hippocampome types, these estimates may be used to generate constraints for optimization. While no such constraints were used to generate the results in this thesis, they may prove useful in future work. A method for generating constraints from molecular marker data is therefore presented.

The form of constraints generated from molecular marker data is the same as those for other stereological counts. An estimate of the number of marker-positive neurons in a particular layer may be equated with the sum of the layer-specific population sizes of all marker-positive types in that layer. For example, an estimate of the number of calbindin-positive neurons in SG is equal to the sum of the SG populations of each neuron type in the dentate gyrus that is positive for calbindin.

$$\text{CB-positive neurons in SG} = \sum \text{CB-positive SG populations}$$

In order for this constraint to be expressed in our parameter scheme, we must substitute its terms with expressions containing only constants and layer-specific type populations. This is only possible under two conditions: **(1)** an estimate is available of the number of CB-positive neurons in SG; this allows the substitution of the left side with a constant. **(2)** the CB expression status of all types with somata in SG is known. This allows the sum on the right side to be substituted with a sum of individual layer-specific type populations. If we do not know the CB expression of a type with somata in SG, then we are uncertain whether to include its population in the sum and therefore cannot express the constraint without introducing additional parameters.

	CB	CR	CCK	nNOS	PV	NPY	SOM	VIP	
DG:H	1058	2075	302	7930	1344	11626	9677	1453	A Estimated neuron count
DG:SG	181	870	293	3790	2055	893	70	707	
DG:SM	480	293	110	7421	370	778	14	168	
DG:H	2/7	2/7	2/7	2/7	2/7	1/7	2/7	0/7	B Fraction of types with known expression
DG:SG	4/11	5/11	5/11	4/11	5/11	3/11	5/11	2/11	
DG:SM	0/5	1/5	4/5	2/5	1/5	2/5	5/5	1/5	

Figure 7.3: Known Marker Expression and Estimates of Layer-Specific Marker-Positive Counts

Figure 7.3A provides estimates of the number of marker-positive neurons in each layer of the dentate gyrus. The rows of the table represent the layers of the dentate gyrus. The columns represent markers. The entries are estimates of the numbers of marker-positive neurons in the corresponding layers. These estimates were derived by multiplying the total GABAergic count for a layer (Buckmaster & Jongen-Relo 1999) with the ratio of marker-positive to GABAergic neurons in that layer (Jinno & Kosaka 2006). Data were not available that distinguished the inner and outer molecular layers.

Figure 7.3B summarizes the available data for the expression of 8 different molecular markers in dentate gyrus Hippocampome types. For each combination of a layer with a marker, there is a fractional entry in the table. The denominator is equal to the total number of neuron types with somata in the layer corresponding to the row. Hence the denominators are the same across each row. The numerator is equal to the number of types with somata in that layer for which the expression status of the column's marker is known. Entries in the table for which the numerator equals the denominator satisfy condition **(2)**. While marker expression data that distinguishes inner and outer molecular layers is available, they have been combined here in order to give B the same tabular structure A. This simplifies the exposition of constraint formation.

Constraints may be generated from these tables as follows:

- for each marker-layer pair for which there exists an entry in A, and for which the entry in B has numerator equal to denominator
 - set the left side of the equation to the entry of A
 - set the right side to the sum of the parameters representing the layer-specific populations for each marker-positive type in the layer

There is only a single entry in Figure 7.3B with numerator equal to denominator. However, all types with somata in this layer are negative. In this case, the above algorithm results in a constraint with no parameters in it (it equates the estimate with 0, since there are no terms in the right side sum), which is not useful. Therefore, with only the data above, no constraints can be formed with the described procedure. This is the reason that none were used in the present study. However, as more information accumulates regarding the marker expression of dentate gyrus Hippocampome types, Figure 7.3B can be updated. When the expression status is known for more marker/layer pairs, then useful constraints may be formed.

7.3 Analysis of Constraints

The equations derived from the data described above yield a system of linear equations. There are 24 total equations and 23 parameters. 13 of the equations come from morphological ratios, 10 come from stereological data, and 1 comes from an assumption. However, several of the equations are not independent, so the system is not fully constrained.

For example, two morphological ratios, Neurogliaform::MOPP and Mossy::QuadMC, have two different versions of the same equation. Both Armstrong et al (2011) and Ceranik et al (1997) provide estimates of the ratio of Neurogliaform to MOPP cells. Similarly, both Buckmaster et al (1992) and Buckmaster (2012) provide ratios of Mossy to QuadMC types. In each case, both equations were included because neither source was deemed more reliable than the other.

The remaining dependent constraints come from stereological data. In the parameter scheme chosen, the maximum number of independent constraints that can come purely from counts and distributions of GABAergic, glutamatergic, and total neurons is 7. These correspond to the GABAergic counts for each layer, and the glutamatergic counts for three layers (SMo has no glutamatergic neurons). These constraints may be obtained by either ratios or counts. 6 out of 7 of these have been ascertained in the literature search of the present study. The ratio of GABAergic neurons between SMo and SMi could not be found.

7.3.1 Constrained and Unconstrained Parameters

(Figure 7.4) shows the row-reduced echelon form of the matrix representation of the system of equations. The rank of this matrix is 18. In the matrix, each column corresponds to a parameter (i.e. a layer-specific population of a neuron type). Rows which contain only a single non-zero entry indicate constrained parameters (one example is shown with a horizontally-oriented blue rectangle in Figure 7.4); the column in which the non-zero entry lies gives the parameter (vertically-oriented blue rectangle). An example of an unconstrained parameter is shown with red rectangles below. Using this approach, the parameters can be

sorted into two categories. In the optimization process, one would expect the unconstrained parameters to vary more than the constrained parameters.

0	A	B	C	D	E	F	G	H	I	J	K	L	M	N	O	P	Q	R	S	T	U	V	W
1	1	0	0	0	0	0	0	0	0	0	0	0	0	0	0	0	0	0	0	0	0	0	0
2	0	1	0	0	0	0	0	0	0	0	0	0	0	0	0	0	0	0	0	0	0	0	0
3	0	0	1	0	0	0	0	0	0	0	0	0	0	0	0	0	0	0	0	0	0	0	0
4	0	0	0	1	1	0	0	0	0	0	0	0	0	0	0	0	0	0	0	0	0	0	0
5	0	0	0	0	0	1	0	0	0	0	0	0	0	0	0	0	0	0	0	0	0	0	0
6	0	0	0	0	0	0	1	0	0	0	0	0	0	1	0	0	0	0	0	0	0	0	0
7	0	0	0	0	0	0	0	1	0	0	0	0	0	1	0	0	0	0	0	0	-1	0	-1
8	0	0	0	0	0	0	0	0	1	0	0	0	0	0	0	0	0	0	0	0	0	0	0
9	0	0	0	0	0	0	0	0	0	1	0	0	0	-1	0	0	0	0	0	0	0	1	0
10	0	0	0	0	0	0	0	0	0	0	1	0	0	0	0	0	0	0	0	0	0	0	1
11	0	0	0	0	0	0	0	0	0	0	0	1	1	0	0	0	0	0	0	0	0	0	0
12	0	0	0	0	0	0	0	0	0	0	0	0	0	0	1	0	0	0	0	0	0	0	0
13	0	0	0	0	0	0	0	0	0	0	0	0	0	0	0	1	0	1	0	0	0	0	0
14	0	0	0	0	0	0	0	0	0	0	0	0	0	0	0	0	1	0	0	0	0	0	0
15	0	0	0	0	0	0	0	0	0	0	0	0	0	0	0	0	0	0	1	0	0	0	0
16	0	0	0	0	0	0	0	0	0	0	0	0	0	0	0	0	0	0	0	1	1	0	1
17	0	0	0	0	0	0	0	0	0	0	0	0	0	0	0	0	0	0	0	0	0	1	0
18	0	0	0	0	0	0	0	0	0	0	0	0	0	0	0	0	0	0	0	0	0	0	0
19	0	0	0	0	0	0	0	0	0	0	0	0	0	0	0	0	0	0	0	0	0	0	0
20	0	0	0	0	0	0	0	0	0	0	0	0	0	0	0	0	0	0	0	0	0	0	0
21	0	0	0	0	0	0	0	0	0	0	0	0	0	0	0	0	0	0	0	0	0	0	0
22	0	0	0	0	0	0	0	0	0	0	0	0	0	0	0	0	0	0	0	0	0	0	0
23	0	0	0	0	0	0	0	0	0	0	0	0	0	0	0	0	0	0	0	0	0	0	0

- | | | | | | |
|---|-----------------------|---|--------------------------|---|----------------------|
| A | DG:H:Hilar Granule | I | DG:SG:Axo-Axonic | Q | DG:SMo:MOPP |
| B | DG:H:Mossy | J | DG:SG:HIPP | R | DG:SMi:Basket-CCK |
| C | DG:H:Quad MC | K | DG:SG:Aspiny Hilar | S | DG:SMo:Neurogliaform |
| D | DG:SG:Granule | L | DG:SG:Basket-PV | T | DG:H:HICAP |
| E | DG:SG:Total Molecular | M | DG:SG:Basket-CCK | U | DG:H:HIPP |
| F | DG:SG:MOLAX | N | DG:SG:Non-Ivy / NGF | V | DG:H:Hilar proj |
| G | DG:SG:Outer Molecular | O | DG:SMi:Semilunar Granule | W | DG:H:Aspiny Hilar |
| H | DG:SG:HICAP | P | DG:SMi:MOPP | | |

Figure 7.4: Row-Reduced Echelon Form

WELL-CONSTRAINED	UNCONSTRAINED
DG:H:Hilar Granule DG:H:Mossy DG:H:Quad MC DG:SG:Granule DG:SG:Total Molecular DG:SG:MOLAX DG:SG:Axo-Axonic DG:SMi:Semilunar Granule DG:SMo:MOPP DG:SMo:Neurogliaform DG:H:Hilar proj	DG:SG:Outer Molecular DG:SG:HICAP DG:SG:HIPP DG:SG:Aspiny Hilar DG:SG:Basket-PV DG:SG:Basket-CCK DG:SG:Non-Ivy / NGF DG:SMi:MOPP DG:SMi:Basket-CCK DG:H:HICAP DG:H:HIPP DG:H:Aspiny Hilar

Figure 7.5: Well-Constrained Parameters

Chapter 8: Results and Discussion

8.1 Description of Results

The optimization algorithm was run with a temperature setting ranging from 130 to 169.5 in 0.5 unit increments, for a total of 80 trials. The results are presented in Figure 8.1. The types that are green have well-constrained parameters; those that are red have poorly-constrained parameters. Orange types have a population in one layer that is well-constrained, and a population in another that is unconstrained. A 95% confidence interval is presented for the mean trial result under the assumption that the results are normally distributed. As expected, well-constrained parameters showed a smaller coefficient of error ($\frac{\sigma}{\mu}$) than did larger parameters.

Name	Layer	95% CI	Mean	Coeff Error	Name	Layer	95% CI	Mean	Coeff Error
Hilar Granule	H/ALL	89–90	89	0.002	Aspiny Hilar	SG	375–669	522	1.286
Mossy	H/ALL	17149–17549	17303	0.053		H	3817–4489	4153	0.364
Quad MC	H/ALL	4084–4471	4314	0.203		ALL	4379–4971	4675	0.284
Granule	SG/ALL	1161163–1175202	1168164	0.029	Basket-PV	SG/ALL	1632–2488	2060	0.933
Total Molecular	SG/ALL	2257–2631	2391	0.359		SG	2282–3083	2682	0.671
MOLAX	SG/ALL	2025–2354	2391	0.354	Basket-CCK	SMI	1761–2365	2063	0.657
Outer Molecular	SG/ALL	88–186	130	1.682		ALL	4211–5281	4746	0.506
	SG	105–262	183	1.908	Non-Ivy / NGF	SG/ALL	93–266	180	2.166
HICAP	H	3210–4256	3733	0.63	Semilunar Granule	SMI/ALL	1541–1686	1613	0.202
	ALL	3402–4432	3917	0.591		SMI	1588–2238	1913	0.763
Axo-Axonic	SG/ALL	784–906	845	0.326	MOPP	SMo	2990–3173	3081	0.134
	SG	144–387	266	2.049		ALL	4632–5357	4994	0.326
HIPP	H	3194–4292	3743	0.659	Neurogliaform	SMo/ALL	4515–4763	4639	0.121
	ALL	3474–4544	4009	0.599	Hilar proj	H/ALL	8235–9157	8696	0.238
					DG TOTAL		1227905–1242179	1235042	0.0260

	Constrained	Mean Coeff Error = 0.184
	Unconstrained	Mean Coeff Error = 1.129
	Mix	

Figure 8.1: Optimization Results

For constrained parameters, these results show reasonably good agreement with the work of Patton and McNaughton (1995) and Dyhrfeld-Johnsen and Soltesz (2007) (cf Section 4.4). However, because both past efforts made many fewer distinctions among neuron types than the Hippocampome, the points of comparison are few.

Type	Patton & McNaughton 1995	Dyhrfeld-Johnsen & Soltesz 2007	Optimization	
Granule	1,000,000	1,000,000	1,161,163 - 1,175,202	
Semilunar Granule			1,541 - 1,686	
Hilar Granule			89 - 90	
Quad MC	30,000	30,000	4,084 - 4,471	
Mossy			17,149 - 17,549	
Total Molecular			2,257 - 2,631	
MOLAX			2,025 - 2,354	
Outer Molecular			88 - 186	
Neurogliaform			4,515 - 4,763	
Aspiny Hilar	15,000 GABAergic peptidergic polymorphic		4,379 - 4,971	
HIPP			12,000	3,474 - 4,544
HICAP			3,000	3,402 - 4,432
IS			3,000	-
Hilar Projecting				8,235 - 9,157
Basket-PV	10,000	10,000	1,632 - 2,488	
Basket-CCK			4,211 - 5,281	
Axo-Axonic	1,000	2,000	784 - 906	
MOPP		4,000	4,632 - 5,357	
Non-Ivy / NGF			93 - 266	

Figure 8.2: Comparison of Results with Past Efforts

8.2 Interpretation of Results

A distinction must be made between the constrained and unconstrained parameters when interpreting the results. Owing to the underconstraint of the system, the optimization solution is a space rather than a single point. The poorly-constrained parameters vary within this space— thus, there is no one value to which optimization should converge for these parameters. As such, the results of optimization for these parameters is not meaningful.

For the well-constrained parameters, however, there exists an optimal parameter setting; in other words, the solution space is invariant with respect to these parameters. If the optimization algorithm is working, then we should expect the mean result to approximate this value.

Even for the well-constrained parameters, however, the quality of the results depends on the quality of the input constraints. Because there are so few constraints here, and many of these constraints contain an unknown degree of bias, the results even for the well-constrained parameters should be regarded with skepticism.

8.3 Reliability of Constraints

The data used in this analysis can be divided into two types: morphological ratios taken from electrophysiological studies in which the neurons were filled after recording, and estimated counts derived from stereological analyses. These two sorts of data have different reliability.

Morphological ratios suffer from the following sources of error:

- Selection bias due to size and robustness of cells. All of the morphological ratios used to generate constraints were taken from experiments where neurons were recorded and filled with biocytin. The selection of such neurons is not random; smaller neurons are less frequently selected due to the difficulty of contacting them, and more fragile neurons are more frequently damaged and discarded in the recording process. To the extent that the comparative soma size and robustness of the membranes of the different types within a region is unknown, there is unknown bias.

- Unknown experimenter selector bias. Some of the experiments that served as sources for morphological ratios selected for neurons visually based on particular criteria. A frequent criterion is “interneuron”. If there are some kinds of interneurons that look stereotypically more “interneuronal” than others, then a selection bias may result.
- The sampling areas used to obtain ratios often did not line up exactly with a Hippocampome parcel. In the presented scheme, however, all ratios were interpreted as applying over a whole parcel.
- The sample size of most ratios is smaller than is desirable.

The stereological counts are much more reliable. Unlike the studies from which the ratios were taken, stereological studies take the specific aim of estimating a count, ratio or density in a target region. While the results of stereological analyses do not always agree, this disagreement is more likely to result from individual, species, or strain differences in the subjects than it is from methodological differences or bias.

8.4 Future Directions

The results presented here demonstrate that the presented pipeline of annotation, conversion into equations, and optimization can produce results. For it to produce useful results, however, requires that the optimization algorithm be provided with more constraints. There are two sources for these future constraints: further data mined from the literature and assumptions.

Both the present literature and future work are likely to yield more useful data. There remains a queue of papers to be mined for morphological ratios. It is also likely that the coming years will see the publication of more precise estimates of the sizes of the total, GABAergic, and GLUTamatergic populations in the dentate gyrus’ layers.

The most promising set of assumptions concerns the molecular marker expression of different Hippocampome types. There is a potentially rich set of constraints to be derived from stereological studies of molecular markers. The formation of these constraints depends

on a clear statement of which types in a layer are marker positive (cf Section 7.2.3). Along the lines of previous efforts (cf Chapter 4), assumptions may be made about the expression status of different classes that allow such a clear statement.

Another assumption to be incorporated is the existence of dentate gyrus neuron types for which the Hippocampome does not yet account. Due to the constraints on the total numbers of neurons in each layer, optimization will assign a higher average count to each type given a smaller number of types. The presented estimates are therefore likely slightly inflated due to the exclusion of as-yet undiscovered types, or types which are too vaguely described for inclusion in the Hippocampome. One example is the interneuron-specific population described by Gulyas (1996), which was incorporated in Dyhrfeld-Johnsen et al's (2007) model but are not represented in the Hippocampome. These neurons may be accounted for by including additional parameters representing "unknown" types in each layer.

Furthermore, a rational scheme is needed for assigning weights to constraints of different reliability. The present study made a crude distinction between morphological ratios and stereological data by weighting them in a 1:5 ratio. This scheme does not capture the differences in reliability among ratios. A weighting scheme based on the confidence intervals (which depend on the sample size) of ratios could begin to remedy this problem.

Finally, the choice of optimization algorithm in this study was preliminary. It is currently unknown whether the algorithm settings used are optimal. The algorithm is implemented in R, a relatively slow language. An implementation in a faster language, such as C or Julia, would allow a much greater number of optimization trials to be run. This would allow many more constraint sets and combinations of algorithm settings to be tested. It will therefore be useful to explore a range of algorithms, parameter settings, and languages in order to find the combination that produces consistent results most efficiently.

Appendix A: Neuron Types of the Dentate Gyrus

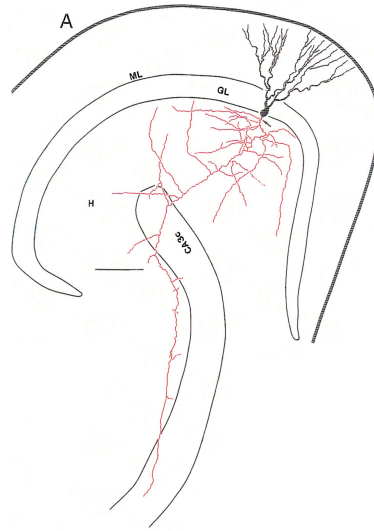


Figure A.1: Granule (+)2201p (Lubke & Spruston 1998)

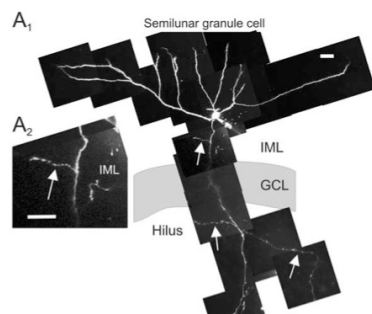


Figure A.2: Semilunar Granule (+)2311p (Williams et al 2010)

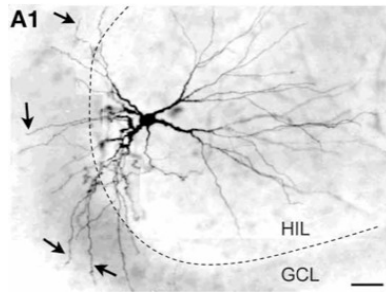


Figure A.3: Quad MC (+)2323 (Scharfman 2012)

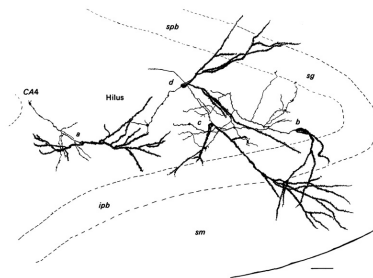


Figure A.4: Hilar Granule (+)2203p (Marti-Subirana et al 1986)

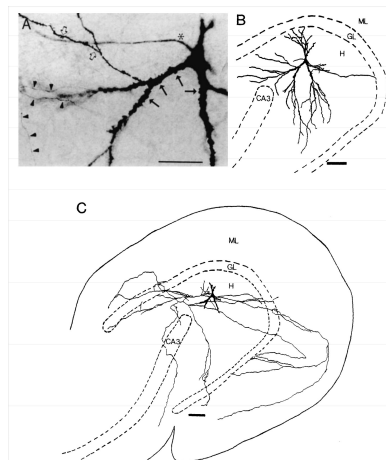


Figure A.5: Mossy (+)0103 (Buckmaster et al 1992)

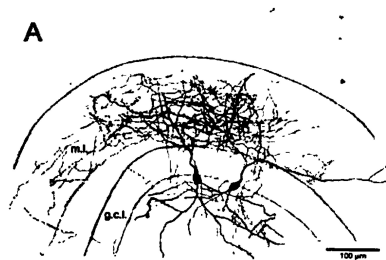


Figure A.6: Total Molecular (-)3303 (Bartos et al 2010)



Figure A.7: MOLAX (-)3302 (Soriano & Frotscher 1993)

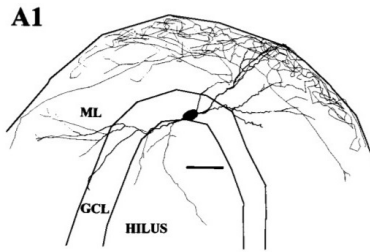


Figure A.8: Outer Molecular (-)3222 (Mott et al 1997)

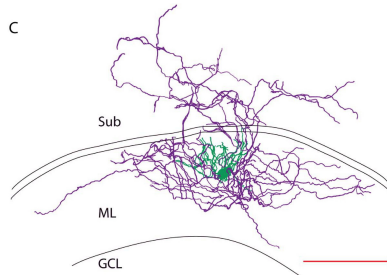


Figure A.9: Neurogliaform (-)3000p (Armstrong et al 2011)

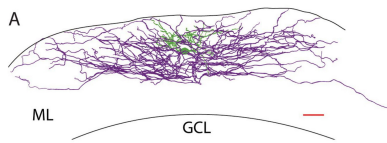


Figure A.10: MOPP (-)3000 (soma SMO) (Armstrong et al 2011)

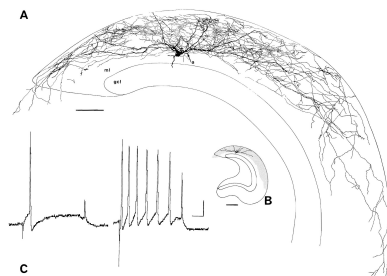


Figure A.11: MOPP (-)3000 (soma SMi) (Han et al 1993)

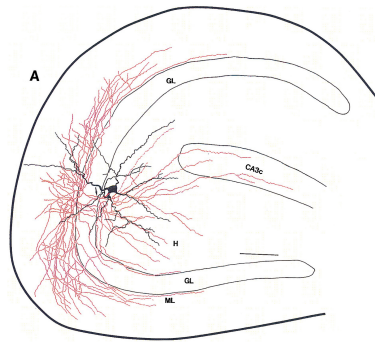


Figure A.12: Aspiny Hilar (-)2333 (Lubke & Spruston 1998)

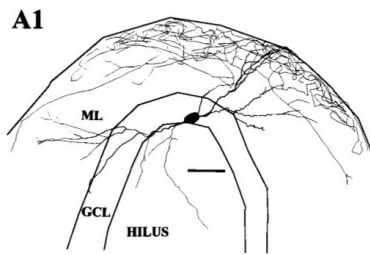


Figure A.13: HICAP (-)2322 (soma SG) (Mott et al 1997)

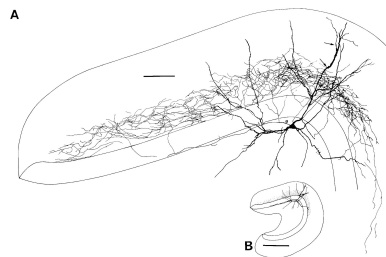


Figure A.14: HICAP (-)2322 (soma H) (Han et al 1993)

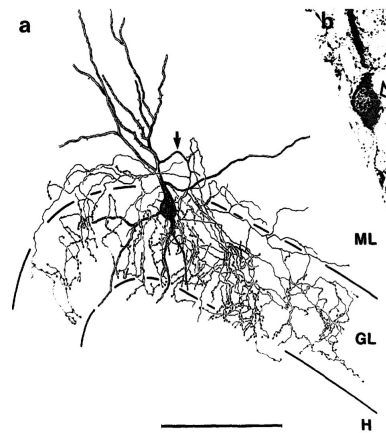


Figure A.15: Axo-Axonic (-)2233 (Soriano & Frotscher 1989)

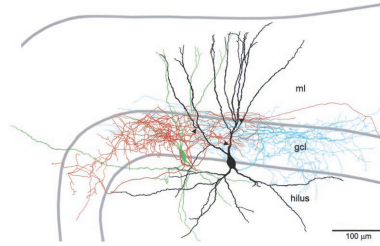


Figure A.16: Basket-PV (-)2232 (Bartos et al 2001)



Figure A.17: Basket-CCK (-)2232 (soma SMi) (Hajos et al 1996)



Figure A.18: Basket-CCK (-)2232 (soma SG) (Hajos et al 1996)

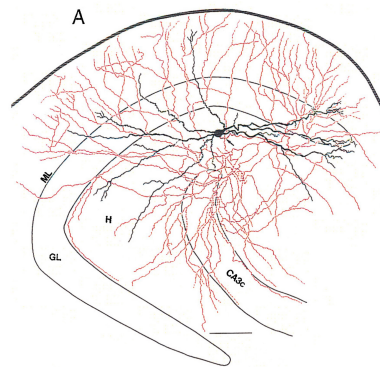


Figure A.19: Hilar proj (-)1333p (Lubke & Spruston 1998)

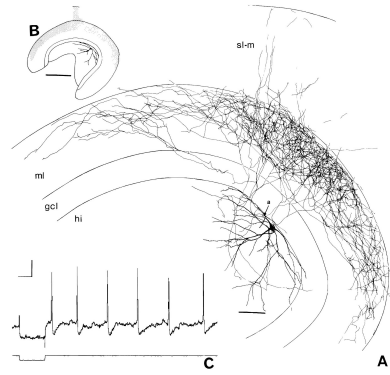


Figure A.20: HIPP (-)1002 (soma SG) (Han et al 1993)

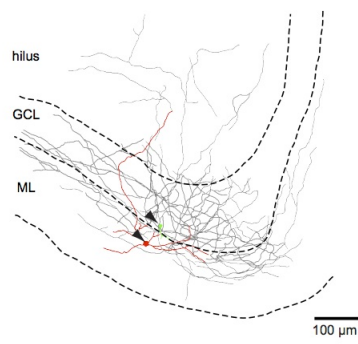


Figure A.21: Non-Ivy / NGF (-)0331 (Markwardt et al 2011)

Appendix B: List of Constraints

B.1 Assumption

B.1.1 Ratio of GABAergic Neurons in SMO:SMi is 2:1

Group Name	Properties	Compatible Types	Final Types
2 DG:SMo	S:DG:SMo GABA+	1007 Neurogliaform (-)3000p 1008 MOPP (-)3000	1007 Neurogliaform (-)3000p 1008 MOPP (-)3000
1 DG:SMi	S:DG:SMi GABA+	1008 MOPP (-)3000 1036 Basket-CCK (-)2232	1008 MOPP (-)3000 1036 Basket-CCK (-)2232

$$\frac{2}{1} = \frac{\text{DG:SMo:Neurogliaform} + \text{DG:SMo:MOPP}}{\text{DG:SMi:MOPP} + \text{DG:SMi:Basket-CCK}}$$

B.2 Morphological Ratio

B.2.1 Armstrong C, Szabadics J, Tamas G, Soltesz I. Neurogliaform cells in the molecular layer of the dentate gyrus as feed-forward gamma-aminobutyric acidergic modulators of entorhinal-hippocampal interplay. *J Comp Neurol* 2011.

Group Name	Properties	Compatible Types	Final Types
11 projecting NGFC	A:SUB A:CA1 nD:SUB nD:CA1 S:DG:SMo A:DG:SMo S:DG:SMoSMi hyperpolarized RMP fast time constant little to no sag during hyperpolarizing pulses late-spiking SLICE:ventral HC dense arborization many en passant boutons	None	1007 Neurogliaform (-)3000p
6 non-projecting NGFC	nD:SUB nD:CA1 nA:CA1 nA:SUB S:DG:SMo A:DG:SMo S:DG:SMoSMi hyperpolarized RMP fast time constant little to no sag during hyperpolarizing pulses late-spiking SLICE:ventral HC dense arborization many en passant boutons	1008 MOPP (-)3000	1008 MOPP (-)3000

$$\frac{11}{6} = \frac{\text{DG:SMo:Neurogliaform}}{\text{DG:SMo:MOPP}}$$

B.2.2 Buckmaster PS, Strowbridge BW, Kunkel DD, Schmiede DL, Schwartzkroin PA. Mossy cell axonal projections to the dentate gyrus molecular layer in the rat hippocampal slice. Hippocampus 1992.

Group Name	Properties	Compatible Types	Final Types
35 mossy with no dendrite in SM	nD:DG:(SMoISMi) D:DG:H S:DG:H large spontaneous EPSPs spike frequency adaptation	1002 Mossy (+)0103 1013 HIPP (-)1002 1026 Hilar proj (-)1333p	1002 Mossy (+)0103
6 mossy with dendrite in SM	D:DG:(SMoISMi) D:DG:H S:DG:H large spontaneous EPSPs spike frequency adaptation	1009 HICAP (-)2322 1026 Hilar proj (-)1333p 1027 Aspiny Hilar (-)2333 1041 Hilar Granule (+)2203p 1043 Quad MC (+)2323	1043 Quad MC (+)2323

$$\frac{35}{6} = \frac{\text{DG:H:Mossy}}{\text{DG:H:Quad MC}}$$

B.2.3 Buckmaster PS. Mossy cell dendritic structure quantified and compared with other hippocampal neurons labeled in rats in vivo. Epilepsia 2012.

Group Name	Properties	Compatible Types	Final Types
3 mossy cells with dendrite in SM	D:DG:(SMo SMi) D:DG:H large somata thorny excrescences on proximal dendrites thick proximal dendrite	1004 Total Molecular (-)3303 1005 MOLAX (-)3302 1006 Outer Molecular (-)3222 1009 HICAP (-)2322 1010 Axo-Axonic (-)2233 1026 Hilar proj (-)1333p 1027 Aspiny Hilar (-)2333 1035 Basket-PV (-)2232 1036 Basket-CCK (-)2232 1041 Hilar Granule (+)2203p 1043 Quad MC (+)2323	1043 Quad MC (+)2323
9 mossy cells without dendrite in SM	nD:DG:SMo nD:DG:SMi D:DG:H large somata thorny excrescences on proximal dendrites thick proximal dendrite	1002 Mossy (+)0103 1013 HIPPI (-)1002 2042 Interneuron Spec (-)03333p	1002 Mossy (+)0103

$$\frac{3}{9} = \frac{\text{DG:H:Quad MC}}{\text{DG:H:Mossy}}$$

B.2.4 Ceranik K, Bender R, Geiger JR, Monyer H, Jonas P, Frotscher M, Lubke J. A novel type of GABAergic interneuron connecting the input and the output regions of the hippocampus. J Neurosci 1997.

Group Name	Properties	Compatible Types	Final Types
14 axons primarily OML	A:DG:SMo nA:CA3:SLM nA:SUB S:DG:SMo axons mainly in SMO resting potential > -50 mV	1008 MOPP (-)3000	1008 MOPP (-)3000
3 axons in CA1:SLM	A:CA3:SLM S:DG:SMo resting potential > -50 mV	None	None
17 axons in SUB	A:SUB A:DG:SMo S:DG:SMo resting potential > -50 mV	1007 Neurogliaform (-)3000p	1007 Neurogliaform (-)3000p
6 granule	D:DG:(SMo SMi) A:DG:H S:DG:SMo round to ovoid somata densely spiny dendrites resting potential > -50 mV	None	None

$$\frac{14}{17} = \frac{\text{DG:SMo:MOPP}}{\text{DG:SMo:Neurogliaform}}$$

B.2.5 Han ZS. Electrophysiological and morphological differentiation of chandelier and basket cells in the rat hippocampal formation: a study combining intracellular recording and intracellular staining with biocytin. Neurosci Res 1994.

Group Name	Properties	Compatible Types	Final Types
6 basket	A:DG:SG S:DG:SGIH extensive axonal arborization fast-spiking perisomatic not spiny sparsely spiny	1010 Axo-Axonic (-)2233 1026 Hilar proj (-)1333p 1027 Aspiny Hilar (-)2333 1035 Basket-PV (-)2232 1036 Basket-CCK (-)2232 1040 Non-lvy / NGF (-)0331	1035 Basket-PV (-)2232 1036 Basket-CCK (-)2232
1 chandelier	A:DG:SG S:DG:SGIH A:DG:H fast-spiking extensive axonal arborization axo-axonic not spiny sparsely spiny	1010 Axo-Axonic (-)2233 1026 Hilar proj (-)1333p 1027 Aspiny Hilar (-)2333 1040 Non-lvy / NGF (-)0331	1010 Axo-Axonic (-)2233
5 axo-dendritic	A:DG:SMIIlSMo S:DG:SGIH extensive axonal arborization fast-spiking dendrite-targeting not spiny sparsely spiny	1002 Mossy (+)0103 1004 Total Molecular (-)3303 1005 MOLAX (-)3302 1006 Outer Molecular (-)3222 1009 HICAP (-)2322 1013 HIPP (-)1002 1026 Hilar proj (-)1333p 1027 Aspiny Hilar (-)2333 1040 Non-lvy / NGF (-)0331 1043 Quad MC (+)2323	1004 Total Molecular (-)3303 1005 MOLAX (-)3302 1006 Outer Molecular (-)3222 1009 HICAP (-)2322 1013 HIPP (-)1002 1026 Hilar proj (-)1333p 1027 Aspiny Hilar (-)2333 1040 Non-lvy / NGF (-)0331

$$\frac{6}{1} = \frac{\text{DG:SG:Basket-PV} + \text{DG:SG:Basket-CCK}}{\text{DG:SG:Axo-Axonic}}$$

$$\frac{1}{5} = \frac{\text{DG:SG:Axo-Axonic}}{\text{DG:SG:Total Molecular} + \text{DG:SG:MOLAX} + \text{DG:SG:Outer Molecular} + \text{DG:SG:HICAP} + \text{DG:H:HICAP} + \text{DG:SG:HIPP} + \text{DG:H:HIPP} + \text{DG:H:Hilar proj} + \text{DG:SG:Aspiny Hilar} + \text{DG:H:Aspiny Hilar} + \text{DG:SG:Non-Ivy / NGF}}$$

B.2.6 Lubke J, Frotscher M, Spruston N. Specialized electrophysiological properties of anatomically identified neurons in the hilar region of the rat fascia dentata. J Neurophysiol 1998.

Group Name	Properties	Compatible Types	Final Types
6 dentate basket cells	D:DG:H D:DG:SMo D:DG:SMi D:DG:SG A:DG:SG nA:DG:SMo nA:DG:SMi nA:DG:H S:DG:H	None	1035 Basket-PV (-)2232 1036 Basket-CCK (-)2232
3 spiny interneurons with projection to the outer molecular layer	D:DG:H A:DG:H A:DG:SMo A:DG:SMi A:CA3:SP S:DG:H	1026 Hilar proj (-)1333p	1026 Hilar proj (-)1333p
4 aspiny interneurons with projection to the inner molecular layer	D:DG:H A:DG:H A:DG:SG A:DG:SMi nA:DG:SMo S:DG:H	1027 Aspiny Hilar (-)2333	1027 Aspiny Hilar (-)2333
4 aspiny interneurons with projection to the outer molecular layer	D:DG:H D:DG:SG A:DG:SMo A:DG:SMi A:DG:H A:DG:SG S:DG:H	1026 Hilar proj (-)1333p	1026 Hilar proj (-)1333p

$$\frac{6}{7} = \frac{\text{DG:SG:Basket-PV} + \text{DG:SG:Basket-CCK}}{\text{DG:H:Hilar proj}}$$

$$\frac{7}{4} = \frac{\text{DG:H:Hilar proj}}{\text{DG:SG:Aspiny Hilar} + \text{DG:H:Aspiny Hilar}}$$

B.2.7 Mott DD, Turner DA, Okazaki MM, Lewis DV. Interneurons of the dentate-hilus border of the rat dentate gyrus: morphological and electrophysiological heterogeneity. J Neurosci 1997.

Group Name	Properties	Compatible Types	Final Types
4 GCL cells	A:DG:SG nA:DG:SMi nA:DG:SMo nA:DG:H S:DG:(SGIH) delicate beaded appearance of axonal arbor aspiny dendrites soma on DG:SG/H border	1035 Basket-PV (-)2232 1036 Basket-CCK (-)2232	1035 Basket-PV (-)2232 1036 Basket-CCK (-)2232
8 IML cells	A:DG:SMi S:DG:(SGIH) aspiny sparsely spiny dendrites axons mostly in SMi soma on DG:SG/H border	1002 Mossy (+)0103 1004 Total Molecular (-)3303 1005 MOLAX (-)3302 1009 HICAP (-)2322 1026 Hilar proj (-)1333p 1027 Aspiny Hilar (-)2333 1040 Non-Ivy / NGF (-)0331 1043 Quad MC (+)2323	1009 HICAP (-)2322 1027 Aspiny Hilar (-)2333 1040 Non-Ivy / NGF (-)0331
6 OML cells	A:DG:SMo S:DG:(SGIH) axons mostly in SMo soma on DG:SG/H border	1004 Total Molecular (-)3303 1005 MOLAX (-)3302 1006 Outer Molecular (-)3222 1013 HIPPP (-)1002 1026 Hilar proj (-)1333p	1006 Outer Molecular (-)3222 1013 HIPPP (-)1002
11 TML cells with axon in H	A:DG:H A:DG:SMo A:DG:SMi S:DG:(SGIH) less dense arborization than IML/OML soma on DG:SG/H border	1004 Total Molecular (-)3303 1026 Hilar proj (-)1333p	1004 Total Molecular (-)3303
11 TML cells with no axon in H	nA:DG:H A:DG:SMo A:DG:SMi S:DG:(SGIH) less dense arborization than IML/OML soma on DG:SG/H border	1005 MOLAX (-)3302	1005 MOLAX (-)3302

$$\frac{4}{8} = \frac{\text{DG:SG:Basket-PV} + \text{DG:SG:Basket-CCK}}{\text{DG:SG:HICAP} + \text{DG:H:HICAP} + \text{DG:SG:Aspiny Hilar} + \text{DG:H:Aspiny Hilar} + \text{DG:SG:Non-Ivy} / \text{NGF}}$$

$$\frac{8}{6} = \frac{\text{DG:SG:HICAP} + \text{DG:H:HICAP} + \text{DG:SG:Aspiny Hilar} + \text{DG:H:Aspiny Hilar} + \text{DG:SG:Non-Ivy} / \text{NGF}}{\text{DG:SG:Outer Molecular} + \text{DG:SG:HIPP} + \text{DG:H:HIPP}}$$

$$\frac{6}{11} = \frac{\text{DG:SG:Outer Molecular} + \text{DG:SG:HIPP} + \text{DG:H:HIPP}}{\text{DG:SG:Total Molecular}}$$

$$\frac{11}{11} = \frac{\text{DG:SG:Total Molecular}}{\text{DG:SG:MOLAX}}$$

B.2.8 Williams PA, Larimer P, Gao Y, Strowbridge BW. Semilunar granule cells: glutamatergic neurons in the rat dentate gyrus with axon collaterals in the inner molecular layer. J Neurosci 2007.

Group Name	Properties	Compatible Types	Final Types
169 fast-spiking	S:DG:SMi fast-spiking	1001 Semilunar Granule (+)2311p 1008 MOPP (-)3000 1036 Basket-CCK (-)2232	1008 MOPP (-)3000 1036 Basket-CCK (-)2232
64 non-fast-spiking	S:DG:SMi non-fast-spiking	1001 Semilunar Granule (+)2311p 1008 MOPP (-)3000 1036 Basket-CCK (-)2232	1001 Semilunar Granule (+)2311p

$$\frac{169}{64} = \frac{\text{DG:SMi:MOPP} + \text{DG:SMi:Basket-CCK}}{\text{DG:SMi:Semilunar Granule}}$$

B.3 Stereology

B.3.1 Buckmaster PS, Jongen-Relo AL. Highly specific neuron loss preserves lateral inhibitory circuits in the dentate gyrus of kainate-induced epileptic rats. *J Neurosci* 1999.

Group Name	Properties	Compatible Types	Final Types
16801 DG:H/GABA+	S:DG:H GABA+	1009 HICAP (-)2322 1013 HIPP (-)1002 1026 Hilar proj (-)1333p 1027 Aspiny Hilar (-)2333	1009 HICAP (-)2322 1013 HIPP (-)1002 1026 Hilar proj (-)1333p 1027 Aspiny Hilar (-)2333

16801 = DG:H:HICAP + DG:H:HIPP + DG:H:Hilar proj+
DG:H:Aspiny Hilar

Group Name	Properties	Compatible Types	Final Types
46734 DG:H	S:DG:H	1002 Mossy (+)0103 1009 HICAP (-)2322 1013 HIPP (-)1002 1026 Hilar proj (-)1333p 1027 Aspiny Hilar (-)2333 1041 Hilar Granule (+)2203p 1043 Quad MC (+)2323	1002 Mossy (+)0103 1009 HICAP (-)2322 1013 HIPP (-)1002 1026 Hilar proj (-)1333p 1027 Aspiny Hilar (-)2333 1041 Hilar Granule (+)2203p 1043 Quad MC (+)2323

46734 = DG:H:Mossy + DG:H:HICAP + DG:H:HIPP+
 DG:H:Hilar proj + DG:H:Aspiny Hilar + DG:H:Hilar Granule+
 DG:H:Quad MC

Group Name	Properties	Compatible Types	Final Types
35900 DG/GABA+	S:DG GABA+	1004 Total Molecular (-)3303 1005 MOLAX (-)3302 1006 Outer Molecular (-)3222 1007 Neurogliaform (-)3000p 1008 MOPP (-)3000 1009 HICAP (-)2322 1010 Axo-Axonic (-)2233 1013 HIPP (-)1002 1026 Hilar proj (-)1333p 1027 Aspiny Hilar (-)2333 1035 Basket-PV (-)2232 1036 Basket-CCK (-)2232 1040 Non-Ivy / NGF (-)0331	1004 Total Molecular (-)3303 1005 MOLAX (-)3302 1006 Outer Molecular (-)3222 1007 Neurogliaform (-)3000p 1008 MOPP (-)3000 1009 HICAP (-)2322 1010 Axo-Axonic (-)2233 1013 HIPP (-)1002 1026 Hilar proj (-)1333p 1027 Aspiny Hilar (-)2333 1035 Basket-PV (-)2232 1036 Basket-CCK (-)2232 1040 Non-Ivy / NGF (-)0331

35900 = DG:SG:Total Molecular + DG:SG:MOLAX + DG:SG:Outer Molecular+
 DG:SMo:Neurogliaform + DG:SMi:MOPP + DG:SMo:MOPP+
 DG:SG:HICAP + DG:H:HICAP + DG:SG:Axo-Axonic+
 DG:SG:HIPP + DG:H:HIPP + DG:H:Hilar proj+
 DG:SG:Aspiny Hilar + DG:H:Aspiny Hilar + DG:SG:Basket-PV+
 DG:SG:Basket-CCK + DG:SMi:Basket-CCK + DG:SG:Non-Ivy / NGF

Group Name	Properties	Compatible Types	Final Types
26 DG:SG/GABA+	S:DG:SG GABA+	1004 Total Molecular (-)3303 1005 MOLAX (-)3302 1006 Outer Molecular (-)3222 1009 HICAP (-)2322 1010 Axo-Axonic (-)2233 1013 HIPP (-)1002 1027 Aspiny Hilar (-)2333 1035 Basket-PV (-)2232 1036 Basket-CCK (-)2232 1040 Non-Ivy / NGF (-)0331	1004 Total Molecular (-)3303 1005 MOLAX (-)3302 1006 Outer Molecular (-)3222 1009 HICAP (-)2322 1010 Axo-Axonic (-)2233 1013 HIPP (-)1002 1027 Aspiny Hilar (-)2333 1035 Basket-PV (-)2232 1036 Basket-CCK (-)2232 1040 Non-Ivy / NGF (-)0331
47 DG:H/GABA+	S:DG:H GABA+	1009 HICAP (-)2322 1013 HIPP (-)1002 1026 Hilar proj (-)1333p 1027 Aspiny Hilar (-)2333	1009 HICAP (-)2322 1013 HIPP (-)1002 1026 Hilar proj (-)1333p 1027 Aspiny Hilar (-)2333
27 DG:SM/GABA+	S:DG:SMoSMi GABA+	1008 MOPP (-)3000 1036 Basket-CCK (-)2232 1007 Neurogliaform (-)3000p	1008 MOPP (-)3000 1036 Basket-CCK (-)2232 1007 Neurogliaform (-)3000p

$$\frac{26}{47} = \frac{\text{DG:SG:Total Molecular} + \text{DG:SG:MOLAX} + \text{DG:SG:Outer Molecular} + \text{DG:SG:HICAP} + \text{DG:SG:Axo-Axonic} + \text{DG:SG:HIPP} + \text{DG:SG:Aspiny Hilar} + \text{DG:SG:Basket-PV} + \text{DG:SG:Basket-CCK} + \text{DG:SG:Non-Ivy / NGF}}{\text{DG:H:HICAP} + \text{DG:H:HIPP} + \text{DG:H:Hilar proj} + \text{DG:H:Aspiny Hilar}}$$

$$\frac{47}{27} = \frac{\text{DG:H:HICAP} + \text{DG:H:HIPP} + \text{DG:H:Hilar proj} + \text{DG:H:Aspiny Hilar}}{\text{DG:SMi:MOPP} + \text{DG:SMo:MOPP} + \text{DG:SMi:Basket-CCK} + \text{DG:SMo:Neurogliaform}}$$

B.3.2 Jiao Y, Nadler JV. Stereological analysis of GluR2-immunoreactive hilar neurons in the pilocarpine model of temporal lobe epilepsy: correlation of cell loss with mossy fiber sprouting. *Exp Neurol* 2007.

Group Name	Properties	Compatible Types	Final Types
90 DG:H/GLUT+/granule_like	S:DG:H GLUT+ granule_like	1002 Mossy (+)0103 1041 Hilar Granule (+)2203p 1043 Quad MC (+)2323	1041 Hilar Granule (+)2203p

90 = DG:H:Hilar Granule

Group Name	Properties	Compatible Types	Final Types
21542 DG:H/GLUT+/large_mossy_like_soma	S:DG:H GLUT+ large_mossy_like_soma	1002 Mossy (+)0103 1041 Hilar Granule (+)2203p 1043 Quad MC (+)2323	1002 Mossy (+)0103 1043 Quad MC (+)2323

21542 = DG:H:Mossy + DG:H:Quad MC

B.3.3 Rapp PR, Gallagher M. Preserved neuron number in the hippocampus of aged rats with spatial learning deficits. Proc Natl Acad Sci U S A 1996.

Group Name	Properties	Compatible Types	Final Types
1200000 DG:SG	S:DG:SG	1000 Granule (+)2201p 1004 Total Molecular (-)3303 1005 MOLAX (-)3302 1006 Outer Molecular (-)3222 1009 HICAP (-)2322 1010 Axo-Axonic (-)2233 1013 HIPP (-)1002 1027 Aspiny Hilar (-)2333 1035 Basket-PV (-)2232 1036 Basket-CCK (-)2232 1040 Non-Ivy / NGF (-)0331	1000 Granule (+)2201p 1004 Total Molecular (-)3303 1005 MOLAX (-)3302 1006 Outer Molecular (-)3222 1009 HICAP (-)2322 1010 Axo-Axonic (-)2233 1013 HIPP (-)1002 1027 Aspiny Hilar (-)2333 1035 Basket-PV (-)2232 1036 Basket-CCK (-)2232 1040 Non-Ivy / NGF (-)0331

1200000 = DG:SG:Granule + DG:SG:Total Molecular + DG:SG:MOLAX+
 DG:SG:Outer Molecular + DG:SG:HICAP + DG:SG:Axo-Axonic+
 DG:SG:HIPP + DG:SG:Aspiny Hilar + DG:SG:Basket-PV+
 DG:SG:Basket-CCK + DG:SG:Non-Ivy / NGF

B.3.4 Woodson W, Nitecka L, Ben-Ari Y. Organization of the GABAergic system in the rat hippocampal formation: a quantitative immunocytochemical study. J Comp Neurol 1989.

Group Name	Properties	Compatible Types	Final Types
100 DG:SG	S:DG:SG	1000 Granule (+)2201p 1004 Total Molecular (-)3303 1005 MOLAX (-)3302 1006 Outer Molecular (-)3222 1009 HICAP (-)2322 1010 Axo-Axonic (-)2233 1013 HIPP (-)1002 1027 Aspiny Hilar (-)2333 1035 Basket-PV (-)2232 1036 Basket-CCK (-)2232 1040 Non-Ivy / NGF (-)0331	1000 Granule (+)2201p 1004 Total Molecular (-)3303 1005 MOLAX (-)3302 1006 Outer Molecular (-)3222 1009 HICAP (-)2322 1010 Axo-Axonic (-)2233 1013 HIPP (-)1002 1027 Aspiny Hilar (-)2333 1035 Basket-PV (-)2232 1036 Basket-CCK (-)2232 1040 Non-Ivy / NGF (-)0331
2 DG:SG/GABA+	S:DG:SG GABA+	1004 Total Molecular (-)3303 1005 MOLAX (-)3302 1006 Outer Molecular (-)3222 1009 HICAP (-)2322 1010 Axo-Axonic (-)2233 1013 HIPP (-)1002 1027 Aspiny Hilar (-)2333 1035 Basket-PV (-)2232 1036 Basket-CCK (-)2232 1040 Non-Ivy / NGF (-)0331	1004 Total Molecular (-)3303 1005 MOLAX (-)3302 1006 Outer Molecular (-)3222 1009 HICAP (-)2322 1010 Axo-Axonic (-)2233 1013 HIPP (-)1002 1027 Aspiny Hilar (-)2333 1035 Basket-PV (-)2232 1036 Basket-CCK (-)2232 1040 Non-Ivy / NGF (-)0331

$$\frac{100}{2} = \frac{\text{DG:SG:Granule} + \text{DG:SG:Total Molecular} + \text{DG:SG:MOLAX} + \text{DG:SG:Outer Molecular} + \text{DG:SG:HICAP} + \text{DG:SG:Axo-Axonic} + \text{DG:SG:HIPP} + \text{DG:SG:Aspiny Hilar} + \text{DG:SG:Basket-PV} + \text{DG:SG:Basket-CCK} + \text{DG:SG:Non-Ivy} / \text{NGF}}{\text{DG:SG:Total Molecular} + \text{DG:SG:MOLAX} + \text{DG:SG:Outer Molecular} + \text{DG:SG:HICAP} + \text{DG:SG:Axo-Axonic} + \text{DG:SG:HIPP} + \text{DG:SG:Aspiny Hilar} + \text{DG:SG:Basket-PV} + \text{DG:SG:Basket-CCK} + \text{DG:SG:Non-Ivy} / \text{NGF}}$$

Group Name	Properties	Compatible Types	Final Types
100 DG:SM	S:DG:SMoISMi	1001 Semilunar Granule (+)2311p 1008 MOPP (-)3000 1036 Basket-CCK (-)2232 1007 Neurogliaform (-)3000p	1001 Semilunar Granule (+)2311p 1008 MOPP (-)3000 1036 Basket-CCK (-)2232 1007 Neurogliaform (-)3000p
42 DG:SM/GABA+	S:DG:SMoISMi GABA+	1008 MOPP (-)3000 1036 Basket-CCK (-)2232 1007 Neurogliaform (-)3000p	1008 MOPP (-)3000 1036 Basket-CCK (-)2232 1007 Neurogliaform (-)3000p

$$\frac{100}{42} = \frac{\text{DG:SMi:Semilunar Granule} + \text{DG:SMi:MOPP} + \text{DG:SMo:MOPP} + \text{DG:SMi:Basket-CCK} + \text{DG:SMo:Neurogliaform}}{\text{DG:SMi:MOPP} + \text{DG:SMo:MOPP} + \text{DG:SMi:Basket-CCK} + \text{DG:SMo:Neurogliaform}}$$

Appendix C: Boundary Conditions

Unless otherwise noted, boundary conditions were calculated according to the following guidelines:

- **(1) when direct count estimates existed for a type**
 - The lower bound was set to 50% of the lowest direct estimate
 - The upper bound was set to 200% of the highest direct estimate
- **(2) when direct count estimates did not exist for a type, and**
 - **(a)** the type was the only glutamatergic or GABAergic type in a compartment
 - * The lower bound was set to 50% of the lowest estimate of the glutamatergic or GABAergic count for that compartment
 - * The upper bound was set to 200% of the highest estimate of the glutamatergic or GABAergic count for that compartment
 - **(b)** the type was not the only glutamatergic or GABAergic type in a compartment
 - * The lower bound was set to 1% of 50% of the lowest estimate of the glutamatergic or GABAergic count for that compartment
 - * The upper bound was set to 200% of the highest estimate of the glutamatergic or GABAergic count for that compartment

The factor of 1% applied in **2a** represents the assumption that no one interneuron type is more than 100 times more populous than any other in the parcel. This is suggested by the compiled morphological ratios (cf Appendix B)

C.1 Granule Cells

- Lower: 300,000; 50% of the lowest estimate of total SG neurons (lowest SG = 600, 000; Schlessinger et al 1975)

- Upper: 4,000,000; 200% of the highest estimate of total SG granule neurons (highest SG = 2,000,000; West et al 1975)

C.2 Hilar Granule Cells

- Lower: 40; 50% of the lowest number estimated for Hilar Granule cells (lowest Hilar Granule = 89; Jiao et al 2007)
- Upper: 2,000; 200% of the highest number estimated for Hilar Granule cells (highest Hilar Granule = 1,000; McCloskey et al 2006)

C.3 Mossy and Quadrilaminar Mossy

- Lower: 150; 1% of 50% of the lowest number estimated for H glutamatergic neurons (lowest H/GLUT⁺ = 30000; Buckmaster et al 1999)
- Upper: 60000; 200% of the highest number estimated for H glutamatergic neurons (*highestH/GLUT⁺* = 30000; Buckmaster et al 1999)

C.4 Semilunar Granule Cells

- Lower: 70; 1% of 50% of the lowest estimate for glutamatergic molecular layer neurons (lowest SM GLUT⁺ = 13400; Woodson et al 1989; Buckmaster et al 1999)
- Upper: 65000; 200% of the highest estimate for glutamatergic molecular layer neurons (highest SM/GLUT⁺ = 32500; Babb et al 1988; Buckmaster et al 1999)

C.5 Interneurons

- Lower: 1% of 50% of the lowest GABAergic estimate for the compartment of the interneuron

- SG: 60; (lowest SG/GABA⁺ = 12000; Woodson et al 1989, Schlessinger et al 1975)
- H: 90; (lowest H/GABA⁺ = 17000; Buckmaster et al 1999)
- SM: 50 (lowest SM/GABA⁺ = 9700; Buckmaster et al 1999)
- Upper: 200% of the highest GABAergic estimate for the compartment of the interneuron
 - SG: 80,000; (highest SG/GABA⁺ = 40000); Woodson et al 1989, West et al 1991)
 - H: 34000; (highest H/GABA⁺ = 17000); Buckmaster et al 1999)
 - SM: 19000 (highest SM/GABA⁺ = 9700); Buckmaster et al 1999)

Parameter	Lower Bound	Upper Bound	Parameter	Lower Bound	Upper Bound
H:Hilar Granule	40	2000	SG:Basket-CCK	60	80000
H:Mossy	150	60000	SG:Non-Ivy / NGF	60	80000
H:Quad MC	150	60000	SMi:Semilunar Granule	50	19000
SG:Granule	300000	4000000	SMi:MOPP	50	19000
SG:Total Molecular	60	80000	SMo:MOPP	50	19000
SG:MOLAX	60	80000	SMi:Axo-Axonic	50	19000
SG:Outer Molecular	60	80000	SMi:Basket-CCK	50	19000
SG:HICAP	60	80000	SMo:Neurogliaform	50	19000
SG:Axo-Axonic	60	80000	H:HICAP	90	34000
SG:HIPP	60	80000	H:HIPP	90	34000
SG:Aspiny Hilar	60	80000	H:Hilar proj	90	34000
SG:Basket-PV	60	80000	H:Aspiny Hilar	90	34000

Figure C.1: Boundary Conditions

Appendix D: Annotation Format

D.1 Annotation Motivation

The goal of annotation was to store an interpretation of a paper that could be used to generate quantitative statements about Hippocampome type populations. Due to the fact that the Hippocampome formally captures only a limited set of neuronal properties, two layers of interpretation were required (cf Section 5.3). The two layers were:

- (1) formal quantitative assertions about specific neuronal populations defined by sets of properties
- (2) formal associations of described neuronal populations with Hippocampome types

Both sorts of interpretation required judgment on the part of the annotator. The annotation files thus needed to capture both the interpretation and its justification.

D.2 Content

There are three kinds of annotation files that associate different kinds of information with groups:

- morphological ratio
- stereological
- type

Morphological ratio and stereological annotation files capture a single quantitative assertion from a single paper. If a paper contains multiple assertions, multiple files must be created. The assertion may be either a ratio of multiple neuron populations or a count of a single population. Within a file, information is associated with neuronal **groups**. A group is a neuronal population described by the authors. An annotation that captures a ratio

must define multiple groups, whereas a count annotation need only define a single group. An annotation associates names, formal and informal neuronal properties (cf Section 2.2), and numbers with these groups. In a morphological ratio file, every association of a property with a group is supported by evidence in the form of a quote, table, or figure.

The definition of groups in stereological papers is much more straightforward than it is in the morphological case. This is because the group is defined purely by location and staining status (interpreted as marker/neurotransmitter expression or, for general neuronal stains, being a neuron as opposed to a glial cell). Because of this reduced complexity, evidence/justification for group definitions are not recorded in marker annotation files.

A type annotation file is designed to be used in concert with one of the other two types of annotations. This file captures an explicit association or dissociation (with justification) of Hippocampome types with the groups defined in the other file.

D.3 Syntax

D.3.1 Design Principles

The annotation syntax was designed with four principles in mind:

1. **efficient data collection and editing** Because group definitions need to be backed with quote/table/figure evidence, there is the potential for annotation files to be large. Copying large quotes multiple times is unpleasant, time-consuming, and error-prone for a human annotator. Therefore, a design that eliminates the need to copy quotes twice was chosen at the cost of additional complexity.
2. **human-readability**
3. **machine-readability**
4. **extensibility** The annotations should be extensible without danger of breaking the code that uses them. The YAML file format used allows the insertion of arbitrary fields. For example, a “notes” field is not required, but can be inserted at any place within an annotations.

D.3.2 Base Format

Annotation files are written in YAML, a flexible, human-readable plain-text data format. YAML was chosen because it is easily manipulated in a text editor (principle (1)) and it is schemaless (principle (4)). YAML files consist of an unlimited number of arbitrary key-value pairs. Keys are strings. Values may be strings, numbers, lists of strings or numbers, or lists of key-value pairs. Because a value may itself be a list of key-value pairs, data may be nested to an arbitrary depth. Nesting is captured in the indentation structure of the file. The YAML website provides further information.

D.3.3 Data Fields by Annotation File Type

Since YAML files are schemaless, all annotations may contain arbitrary data. However, the code that interprets the annotations imposes a “soft schema” in that it requires certain fields to be present in each kind of annotation file (while ignoring other fields). A particularly important field in all files is the **groups** field. Required and suggested fields for each type are detailed below. Because the structure of the **groups** field is more complex than the others, the description for **groups** comes after the description of all other fields.

Non-groups Fields

All Annotation Files

- **fly_form** stands for “first_author, last_author, year”. Not required, but very useful for human readers.
- **pmid** PubMed id. Required.
- **notes** for arbitrary comments by the annotator. May be specified as an array or as a single string. Not required but .

Morphological Ratio Files

- **sampled_parcel**s the Hippocampome parcels from which the neurons described in

this annotation were taken. Should be specified as an array.

- **ratio** contains the actual ratio; should contain a sub-field called **numbers**, which contains a list. The elements of the list should be strings consisting of a number followed by a group name. It is important that these group names exactly match the groups defined under **groups**.

Stereology Files

- **weight** The weight of the constraint that will be derived from this observation in the optimization scheme
- **number_type** Either “ratio” or “count”.

Type Files There are no required or suggested fields specific to type files.

The groups Field

The **groups** field is the core of all annotation files. It contains a list of group entries, each of which associates information with a particular neuronal group described in the annotated paper. The required fields of a group entry vary by annotation type. In morphological ratio files, a group entry associates a set of properties with the name of a neuronal population, as well as associated evidence in the form of table/figure references and/or clipped quotes. In a stereology file, a group entry associates properties and a number with a name. No evidence is recorded. In a type file, a group entry associates or dissociates a name with Hippocampome types. A justification for these decisions is also recorded.

Because the groups described in a paper often share many properties, a “flat” annotation scheme in which each group is separately and completely defined is frequently redundant. It is also labor-intensive, since group definition for morphological ratios requires the recording of evidence. While the code can handle such a flat list of groups, it also supports the definition of a taxonomy of groups. The taxonomy is defined by a tree structure made possible by YAML’s arbitrary nesting of data. Groups are the nodes in the tree; child

nodes inherit all the properties of higher-up nodes. The tree is implemented by allowing group entries to themselves contain a **groups** field that defines their subgroups. **groups** may contain a flat list, a single tree, or multiple trees.

The fields for a group entry in each annotation type are detailed below.

All Annotation Files

- **name** the name of the group. When two annotation files reference the same groups in the same paper, it is important that they use exactly the same names. This is because the data contained in the files must be merged by the code in order to generate a final mapping of groups to Hippocampome types. The name is used for the merging.
- **groups** an array of subgroups for the current group. The entries in this field have the same structure as the parent group. Thus the specification for a group entry is recursive.

Morphological Ratio Files

- **evidence** an array of evidence specifications. Each entry represents a particular quote/table/figure and comes with an interpretation asserting that this quote/table/figure is evidence for the containing neuronal group's possession of certain properties. Each evidence entry has fields:
 - **location** page number and location of the quote/table/figure
 - **quote**, **table**, or **figure**. Only the field corresponding to the evidence type should be used. For a table or figure, this should be a simple reference, e.g. "Table 5". For a quote, it should be text clipped from the paper.
 - **properties** an array of properties that the quote/table/figure asserts

Stereology Files

- **properties** a list of properties. These may be either formal or informal properties. See below for a specification of formal properties.

- **number** the count or percentage associated with this group

Type Files

- **include** an array of types to include in the group
- **exclude** an array of types to exclude from the group

The **include** and **exclude** keys contain arrays of type entries. Each entry has two keys:

- **type** the id number of the type followed by a name. The name need not exactly match the name of the Hippocampome type (it will be discarded by code), but the number must be accurate.
- **justification** the reason this type is being included/excluded from this group. This key is not read by code.

Appendix E: Annotation Samples

E.1 Morphological Ratio File

:fly_form: Mott and Lewis 1997

:pmid: 9151716

:notes: |-

The primary breakdown in this ratio is by where arborization is densest. There is considerable variation within each of the groups.

:sampled_parcel:

- DG:SG

- DG:H

:ratio:

:numbers:

- 8 IML cells

- 4 GCL cells

- 6 OML cells

- 11 TML cells with axon in H

- 11 TML cells with no axon in H

:groups:

- :name: all

:evidence:

- :location: 3992 right

:quote: |-

Electrophysiological data were obtained from >60 D/H border interneurons. Of these, we were able to retrieve good

biocytin stains of the axons, dendrites, and somata of 27 cells. In an additional 14 cells, there was incomplete staining of the soma and dendritic tree, usually because of loss or lysis of the soma. In these 14 cells, however, there was adequate axon staining to determine axonal distribution in the molecular layer (ML) or granule cell layer (GCL). Thus, in 41 of the interneurons studied, the axon distribution could be determined. We chose to group D/H border zone interneurons by the distribution of their axons, which has been a key feature in classifying these cells (Han et al., 1993; Halasy and Somogyi, 1993; Buckmaster and Schwartzkroin, 1995a,b). Thus, the 41 neurons with adequate axonal staining were grouped into four morphological classes as follows.

:properties:

- S:DG:(SG|H)
- soma on DG:SG/H border

:groups:

- :name: GCL cells

:evidence:

- :location: 3992 right

:quote: |-

An axon arbor consisting of a delicate net-like arborization in the GCL (Amaral, 1978; Ribak and Seress, 1983; Hart et al., 1993) was recovered in only four cells or ~10% of the 41 cells with defined axonal domains (Fig. 1). The axon arborizations of these cells in the GCL had a delicate beaded appearance, and the branches of the axon were almost

entirely confined to the GCL. In one cell, the soma and dendrites were exceptionally well preserved and it had the typical appearance of a pyramidal basket cell with a prominent apical dendrite. In one other, the soma and portions of the dendrites were recovered, showing that the soma was at the D/H border and dendrites extended into the hilus and ML. The dendrites of these cells were aspiny and varicose. Basket cells and axo-axonic cells are difficult to discern (Han et al., 1993), and we cannot be certain that all of these cells were basket cells rather than being a mix of basket cells and axo-axonic cells, and therefore these cells will be designated GCL cells. Axo-axonic cells, however, often have extensive axonal branching in the hilus as well as in the GCL (Han et al., 1993), favoring the interpretation that these GCL cells, which did not have extensive hilar axons, were indeed basket cells.

:notes:

- |-

'almost entirely confined to SG' has been interpreted as no axons anywhere else

:properties:

- A:DG:SG

- nA:DG:SMi

- nA:DG:SMo

- nA:DG:H

- delicate beaded appearance of axonal arbor

- aspiny dendrites

- :name: IML cells

:evidence:

- :location: 3992 bot right

:quote: |-

Eight cells had axons arborizing predominantly in the IML (Figs. 2, 3). In most cases, the axons arose from apical dendrites, although in one case (Fig. 2) the axon clearly arose from the soma and ascended through the GCL to the IML. Soma shape was fusiform (n = 5) or pyramidal (n = 2) when the soma was visualized. The long axis of the fusiform cell soma could be parallel to the hilar border or, if the soma was embedded in the lower margin of the GCL, vertically oriented. Dendrites were aspiny (six cells) or sparsely spiny (two cells). Most of these cells also had several major dendrites ascending vertically from the soma to enter the ML directly. Occasional branches of the axons of the IML cells often entered the GCL but did not form the extensive and dense network of terminals in the GCL typical of the GCL cells, although one IML cell had a relatively large amount of axon in the GCL (Fig. 3C) similar to an interneuron innervating the IML described by Sik et al. (1997).

:properties:

- A:DG:SMi

- axons mostly in SMi

- aspiny | sparsely spiny dendrites

- :name: OML cells

:evidence:

- :location: 3993 top left

:quote: |-

Six cells had axons that seemed to arborize preferentially in the outer half of the ML and are referred to as OML cells. Unfortunately, the soma and dendrites were well preserved in only two of these cells (Fig. 4). In one cell the axon arose from an ML dendrite and in the other cell it arose from the soma. Both cells had fusiform somata with aspiny dendrites entering both the hilus and ML and extending to the OML.

:properties:

- A:DG:SMo

- axons mostly in SMo

- :name: TML cells

:evidence:

- :location: 3993 bottom left

:quote: |-

This was the most frequently encountered pattern in which the axon originated from an apical dendrite and branched in the ML with no clear concentration in any specific stratum of the ML (Fig. 5). Of the 41 stained axonal arborizations, 22 showed this pattern, and, of these, 17 had adequately stained somatodendritic morphology as well. Compared with the IML and OML cells, the axonal arborization of these cells was not as dense and in many cases branches seemed to wander randomly over the entire thickness of the ML. In general, the axonal arborization was most concentrated in the ML directly overlying the soma, and in occasional cases the axon arborization extended widely in the transverse plane as well, occasionally nearly to the limits of the ML

in both the suprapyramidal and infrapyramidal direction.

Eleven of the TML cells also had axon branches entering the hilus.

:properties:

- A:DG:SMo
- A:DG:SMi
- less dense arborization than IML/OML

:groups:

- :name: TML cells with axon in H

:evidence:

- :location: 3993 bottom left

:quote: |-

Eleven of the TML cells also had axon branches entering the hilus.

:properties:

- A:DG:H

- :name: TML cells with no axon in H

:evidence:

- :location: 3993 bottom left

:quote: |-

Eleven of the TML cells also had axon branches entering the hilus.

:properties:

- nA:DG:H

E.2 Stereology File

:fly_form: Rapp and Gallagher 1996

```
:pmid: 8790433
:number_type: count
:weight: 5
:groups:
- :name: DG:SG
  :parcels:
  - DG:SG
  :properties:
  - S:DG:SG
  :number: 1200000
```

E.3 Type File

```
:fly_form: Mott and Lewis 1997
:pmid: 9151716
:notes:
- |-
  One needs to beware here of types that have somata in
  DG:SG/H but are not found in the border region. They should
  be excluded from these groups, because these cells were
  taken specifically from the border.
- |-
  The primary criterion used to define the authors' groups is
  the density of axonal arborization within a particular
  region.
:groups:
- :name: all
  :exclude:
```

```

- :type: 1026 DG hilar proj
  :justification: |-
    Hilar projecting neurons, while included by the automated
    mapping algorithm, were excluded from all groups for two
    reasons. First, no projections to CA3 are described by Mott
    and Lewis. First, these neurons project to CA3 and no
    projections are mentioned by the authors. Furthermore, it
    is unknown whether these neurons reside at the SG/H border.
    The only known example shows a soma located deeper within
    the hilus, and the authors state that "[these neurons]
    usually had somata in the deep hilus" (cf. "aspiny hilar
    interneurons with axonal projections to the outer molecular
    layer", Lubke et al 1998).

- :name: IML cells
  :exclude:
- :type: 1002 DG Mossy
  :justification: |-
    mossy cells have thick spines on proximal dendrites
    (Scharfman 2012 review of mossy)
- :type: 1043 Quad MC
  :justification: |-
    mossy cells have thick spines on proximal dendrites
    (Scharfman 2012 review of mossy)
- :name: TML cells with axon in H
  :include:
- :type: 1004 DG total molecular
  :justification: |-
    It is possible that some of the neurons classified by Mott

```

and Lewis as OML and IML might be classified in the Hippocampome as MOLAX or Total Molecular. This is because the axons of IML and OML neurons were said to exist \"predominantly\" in the SMi or SMO, respectively-- it is not clear that all of these neurons lacked, by Hippocampome standards, axons in the other part of the molecular layer. Nonetheless, for simplicity, MOLAX and Total Molecular neurons were assigned exclusively to the TML group.

- :name: TML cells with no axon in H

:include:

- :type: 1005 DG MOLAX

:justification: |-

It is possible that some of the neurons classified by Mott and Lewis as OML and IML might be classified in the Hippocampome as MOLAX or Total Molecular. This is because the axons of IML and OML neurons were said to exist \"predominantly\" in the SMi or SMO, respectively-- it is not clear that all of these neurons lacked, by Hippocampome standards, axons in the other part of the molecular layer. Nonetheless, for simplicity, MOLAX and Total Molecular neurons were assigned exclusively to the TML group.

Appendix F: Literature Search Records

Below are presented two tables and two lists of PubMed IDs. The tables capture all articles that had their full text evaluated for the presence of morphological ratios or stereological data. Similar tables are available for all articles that had their abstracts evaluated, but for brevity only lists of PubMed IDs are presented here. For the full literature search dataset, including the list of queries run, contact the author.

F.1 Publications Completely Mined for Citations of Interest

- Dyhrfeld-Johnsen, J., Santhakumar, V., Morgan, R. J., Huerta, R., Tsimring, L., & Soltesz, I. (2007). Topological determinants of epileptogenesis in large-scale structural and functional models of the dentate gyrus derived from experimental data. *Journal of neurophysiology*, 97(2), 1566–1587. doi:10.1152/jn.00950.2006
- Houser, C. R. (2007). Interneurons of the dentate gyrus: an overview of cell types, terminal fields and neurochemical identity. *Progress in brain research*, 163, 217–232. doi:10.1016/S0079-6123(07)63013-1
- Morgan, R. J., Santhakumar, V., & Soltesz, I. (2007). Modeling the dentate gyrus. *Progress in brain research*, 163, 639–658. doi:10.1016/S0079-6123(07)63035-0
- Patton, P. E., & McNaughton, B. (1995). Connection matrix of the hippocampal formation: I. The dentate gyrus. *Hippocampus*, 5(4), 245–286. doi:10.1002/hipo.450050402

F.2 Abstracts Evaluated for Morphological Ratios

17475251, 7889124, 10769252, 10384982, 9527888, 9463463, 9284057, 9284056, 9284055, 9305828, 9065516, 8986870, 8985706, 8841885, 8856701, 8816250, 8871784, 8739155, 8804046, 8620918, 10196544, 10747186, 10777798, 10995835, 11067982, 11226691, 11784700, 11807843, 12096061, 12373367, 12614688, 12625464, 14750656, 15342722, 15498801, 15927687, 16158978,

16237182, 16280590, 16930755, 17016818, 17699661, 17765711, 18504292, 18558471, 18662340, 19189715, 19300446, 19750211, 20130170, 20399728, 20454678, 20510860, 20660272, 20720120, 20882544, 21172609, 21795545, 22161956, 22162008, 22230770, 10036272, 17593972, 17924526, 22633895, 13679415, 12611982, 12367604, 11956340, 20463218, 17287497, 15269966, 20824730, 20433901, 20087886, 19965717, 19496174, 19052205, 19020015, 18216229, 17177260, 17082230, 16455686, 16407558, 16158066, 15772233, 15019577, 14999062, 12684462, 12657704, 12612034, 11906698, 11306622, 11245688, 10805688, 10747187, 10687182, 10601455, 9819247, 9819241, 9763458, 9636096, 9463467, 9502804, 9497075, 9457638, 9401968, 9356400, 9334386, 9307110, 9120580, 7605636, 7520482, 18077672, 17945424, 17935893, 17706254, 17521341, 17459425, 17442771, 17441992, 17389682, 17389682, 8846092, 8848093, 8596652, 8592201, 7560290, 7666147, 7751946, 7643175, 7620614, 7542423, 7874517, 7931561, 7951690, 8173959, 1401262, 1360155, 1381418, 1279453, 1376455, 1348084, 2605525, 22612804, 21455997, 20554881, 19539612, 19535596, 19020040, 17717699, 16685708, 15800071, 15708475, 15261095, 12837565, 12000120, 11423098, 11164792, 11135261, 11113509, 11064364, 10999513, 10902894, 10746247, 10677627, 10594654, 10579567, 9875530, 9450537, 9331177, 9212280, 8101227, 8261117, 7516510, 8035215, 7931512, 7878486, 7550611, 7823179, 7582114, 8542057, 8698887, 8871221, 9228528, 9287083, 9347352, 9104599, 9151716, 9204922, 9184122, 9300764, 12437591, 16431028, 19071166, 19549869, 9503336, 9497429, 10482760, 10655521, 11157084, 11168548, 11920713, 12151544, 12605903, 16641241, 16819624, 18461605, 19109487, 19767413, 19906972, 20363598, 20631216, 21983681, 22125513, 22442084, 23144890, 1284975, 7680800, 8261118, 8394905, 8283200, 8309524, 7897400, 7524961, 7721998, 7656417, 7582089, 8815206, 8895886, 8912906, 9347353, 8576427, 22612815, 22245503, 21344409, 15118092, 15191798, 15776443, 16650619, 18215230, 18780780, 21878933, 23223307, 7119174, 3676805, 1319481, 8895892, 10456092, 9703026, 10999540, 11391638, 11958865, 14753509, 16099669, 16600515, 17662262, 17898215, 18000818, 18189310, 18215229, 15269228, 14580952, 12815027, 11440806, 11246147, 11160382, 21204820, 22960310, 8269038, 8589793, 7472322, 8719345, 9051258, 9051259, 9427485, 9852317, 10579566, 11110821, 12927199, 23419891, 21452204, 20673826, 20037579, 20034063, 19368833, 19270346, 18727953, 18390190, 18221525, 18077687, 17765725, 17765721, 17503488,

17399691, 17360923, 16687493, 11532248, 11541865, 11553300, 11734359, 11734656, 11778053,
11976392, 11976757

F.3 Full Text Evaluated for Morphological Ratios

First/Last Authors & Year	PMID	Title	Relevant	Note
Amaral DG and Lavenex P 2007	17765709	The dentate gyrus: fundamental neuroanatomical organization (dentate gyrus for dummies).	n	review
Ambrogini P and Cuppini R 2004	15261095	Morpho-functional characterization of neuronal cells at different stages of maturation in granule cell layer of adult rat dentate gyrus.	n	This paper contains significant subgroups of granule cells (both morphological and electrophysiological), but this distinction is at a finer grain than is needed for the Hippocampome
Babb TL and Brown WJ 1988	3209750	Distribution of glutamate-decarboxylase-immunoreactive neurons and synapses in the rat and monkey hippocampus: light and electron microscopy.	n	
Blaabjerg M and Zimmer J 2007	17765713	The dentate mossy fibers: structural organization, development and plasticity.	n	
Blasco-Ibanez JM and Freund TF 2000	11043552	Recurrent mossy fibers preferentially innervate parvalbumin-immunoreactive interneurons in the granule cell layer of the rat dentate gyrus.	n	looks at targets of recurrent mossy fiber collaterals
Buckmaster PS 2012	22612804	Mossy cell dendritic structure quantified and compared with other hippocampal neurons labeled in rats in vivo.	y	contains a good examination of the dendrites of mossy cells, which can provide a ratio between Quad MC and normal mossy
Buckmaster PS and Jongen-Relo AL 1999	10531454	Highly specific neuron loss preserves lateral inhibitory circuits in the dentate gyrus of kainate-induced epileptic rats.	n	no reconstructions
Buckmaster PS and Schwartzkroin PA 1992	1284975	Mossy cell axonal projections to the dentate gyrus molecular layer in the rat hippocampal slice.	y	ratio of mossy cell subgroups

Buckmaster PS and Schwartzkroin PA 1995	7823179	Interneurons and inhibition in the dentate gyrus of the rat in vivo.	n	while 44 total neurons were labeled in this study, many of them were granule cells and pyramidal cells; the only potential ratio would be between mossy cells and 2 different kinds of interneuron groups, but the n for the two interneuron groups is extremely low (2 and 3), and it's not clear at all that mossy cells were selected from the same pool (so the ratio between the interneurons and mossy may not be valid). Therefore, this is being shelved for now.
Buckmaster PS and Schwartzkroin PA 1996	8698887	Axon arbors and synaptic connections of hippocampal mossy cells in the rat in vivo.	n	They looked at 11 mossy cells but they were all from
Buhl EH and Somogyi P 1994	8035215	Physiological properties of anatomically identified axo-axonic cells in the rat hippocampus.	n	while they filled a bunch of cells, they selected a subset of them by visual inspection as axo-axonic and provide no information about the others. within the axo-axonic group, no meaningful morphological subgroups are defined.
Bullis JB and Poolos NP 2007	17185334	Reversed somatodendritic I(h) gradient in a class of rat hippocampal neurons with pyramidal morphology.	y	ratio of pyramidal to PLP-RGC neurons
Cameron MC and Nadler JV 2011	21455997	Morphologic integration of hilar ectopic granule cells into dentate gyrus circuitry in the pilocarpine model of temporal lobe epilepsy.	n	all rats in this study were given pilocarpine (even the controls– these were just rats given pilocarpine that did NOT develop status epilepticus)
Canto CB and Witter MP 2008	18769556	What does the anatomical organization of the entorhinal cortex tell us?	n	
Ceranik K and Lubke J 1997	9204922	A novel type of GABAergic interneuron connecting the input and the output regions of the hippocampus.	y	This contains a good ratio of OML interneurons

Daw MI and McBain CJ 2009	19741117	Asynchronous transmitter release from cholecystokinin-containing inhibitory interneurons is widespread and target-cell independent.	n	They did fill cells with biocytin but I do not see a breakdown by number of individual morphological types and the sampling methodology is unclear, so this is not being annotated for now.
Dyhrfeld-Johnsen J and Soltesz I 2007	17093119	Topological determinants of epileptogenesis in large-scale structural and functional models of the dentate gyrus derived from experimental data.	n	modeling
Esclapez M and Houser CR 1995	7700525	Somatostatin neurons are a subpopulation of GABA neurons in the rat dentate gyrus: evidence from colocalization of pre-prosomatostatin and glutamate decarboxylase messenger RNAs.	n	
Fuentealba P and Klausberger T 2008	18367092	Ivy cells: a population of nitric-oxide-producing, slow-spiking GABAergic neurons and their involvement in hippocampal network activity.	n	
Fuentealba P and Somogyi P 2008	18829959	Rhythmically active enkephalin-expressing GABAergic cells in the CA1 area of the hippocampus project to the subiculum and preferentially innervate interneurons.	n	only a single cell is morphologically characterized
Ganter P and Somogyi P 2004	15098728	Properties of horizontal axo-axonic cells in stratum oriens of the hippocampal CA1 area of rats in vitro.	y	ratio of horizontal SO interneurons
Gloveli T and Buhl EH 2005	15486016	Differential involvement of oriens/pyramidal interneurons in hippocampal network oscillations in vitro.	y	percent of O-LM in CA3 SR and SP and some other interneuron type ratios
Gloveli T and Kopell NJ 2005	16141320	Orthogonal arrangement of rhythm-generating microcircuits in the hippocampus.	n	while there were biocytin fillings and recordings, the n was very small (12)
Hajos N and Freund TF 2004	15483131	Spike timing of distinct types of GABAergic interneuron during hippocampal gamma oscillations in vitro.	y	ratio for CA3 interneurons

Halasy K and Somogyi P 1993	8261118	Subdivisions in the multiple GABAergic innervation of granule cells in the dentate gyrus of the rat hippocampus.	n	this is a study of the termination sites of the axons from the neurons described in PMID: 8261117 (Han 1993); see this paper for possible ratios
Hamam BN and Alonso AA 2002	12209840	Morphological and electrophysiological characteristics of layer V neurons of the rat lateral entorhinal cortex.	y	solid study that actually aimed at morphological characterization and comprehensive sampling of EC:V neurons
Hamam BN and Amaral DG 2000	10713573	Morphological and electrophysiological characteristics of layer V neurons of the rat medial entorhinal cortex.	y	ratio of EC:V types (MEC)
Han ZS 1994	7516510	Electrophysiological and morphological differentiation of chandelier and basket cells in the rat hippocampal formation: a study combining intracellular recording and intracellular staining with biocytin.	y	basket to axo-axonic ratio in the DG
Han ZS and Somogyi P 1993	8261117	A high degree of spatial selectivity in the axonal and dendritic domains of physiologically identified local-circuit neurons in the dentate gyrus of the rat hippocampus.	y	ratios of interneurons identified electrophysiologically from across all of DG, but extremely low n
Harris E and Stewart M 2001	11259758	Propagation of synchronous epileptiform events from subiculum backward into area CA1 of rat brain slices.	n	no reconstructions
Harris E and Stewart M 2001	11406828	Intrinsic connectivity of the rat subiculum: I. Dendritic morphology and patterns of axonal arborization by pyramidal neurons.	y	There is morphological classification with numbers of subicular neurons here
Hosseini-Sharifabad M and Nyengaard JR 2007	17368561	Design-based estimation of neuronal number and individual neuronal volume in the rat hippocampus.	n	
Jaffe DB and Gutierrez R 2007	17765714	Mossy fiber synaptic transmission: communication from the dentate gyrus to area CA3.	n	

Jinno S and Kosaka T 2010	19655319	Stereological estimation of numerical densities of glutamatergic principal neurons in the mouse hippocampus.	n	
Klausberger T 2009	19735288	GABAergic interneurons targeting dendrites of pyramidal cells in the CA1 area of the hippocampus.	n	
Klausberger T and Somogyi P 2008	18599766	Neuronal diversity and temporal dynamics: the unity of hippocampal circuit operations.	n	
Larimer P and Strowbridge BW 2010	20037579	Representing information in cell assemblies: persistent activity mediated by semilunar granule cells.	n	they recorded from a large number of semilunar granule cells but apparently they didn't fill them. Not sure how they confirmed them as SGCs, but I'm sure it is in the article if one reads it more closely. But there certainly are not reconstructions, so this is not useful for a ratio
Lee SH and Soltesz I 2010	20534847	Distinct endocannabinoid control of GABA release at perisomatic and dendritic synapses in the hippocampus.	y	There is a ratio between SCA-ADI and CCK+BC in CA1
Leranth C and Hajszan T 2007	17765712	Extrinsic afferent systems to the dentate gyrus.	n	
Losonczy A and Nusser Z 2004	14734812	Persistently active cannabinoid receptors mute a subpopulation of hippocampal interneurons.	n	some sampling of CA3 interneurons but very small sample size, so not used for now
Lubke J and Spruston N 1998	9497429	Specialized electrophysiological properties of anatomically identified neurons in the hilar region of the rat fascia dentata.	y	contains good ratio of interneuron types in DG:H
McCloskey DP and Scharfman HE 2006	17042797	Stereological methods reveal the robust size and stability of ectopic hilar granule cells after pilocarpine-induced status epilepticus in the adult rat.	n	

Mercer A and Thomson AM 2007	17611285	Characterization of neurons in the CA2 subfield of the adult rat hippocampus.	y	sample of CA2 interneurons from CA2:SP with three-way classification
Morgan RJ and Soltesz I 2007	17765743	Modeling the dentate gyrus.	n	none
Mott DD and Lewis DV 1997	9151716	Interneurons of the dentate-hilus border of the rat dentate gyrus: morphological and electrophysiological heterogeneity.	y	good ratio of interneurons from dentate-hilus border
Mott DD and Lewis DV 1999	10482760	GABAB-Receptor-mediated currents in interneurons of the dentate-hilus border.	n	While they did fill a bunch of interneurons from the DG:H/SG border and classify them, they frustratingly do not give the actual numbers of each type identified. However, there is a similar paper by Mott from 1997 that looks at the same sorts of cells and does provide the ratio.
Naber PA and Witter MP 2001	11345131	Reciprocal connections between the entorhinal cortex and hippocampal fields CA1 and the subiculum are in register with the projections from CA1 to the subiculum.	n	no quantitative morphological classification
O'Mara SM and Gigg J 2001	11240210	The subiculum: a review of form, physiology and function.	n	review
Okazaki MM and Nadler JV 1995	7721998	Hippocampal mossy fiber sprouting and synapse formation after status epilepticus in rats: visualization after retrograde transport of biocytin.	n	only covers granule cells and there is no significant morphological subgrouping among the controls
Penttonen M and Buzsaki G 1997	9287083	Feed-forward and feed-back activation of the dentate gyrus in vivo during dentate spikes and sharp wave bursts.	n	Only 2 interneurons were examined, and their anatomy is not even described in this paper (it is in Sik 1997); the rest of the cells are granule and pyramidal, therefore not useful for ratios
Poolos NP and Roth MK 2006	16870744	Modulation of h-channels in hippocampal pyramidal neurons by p38 mitogen-activated protein kinase.	n	study of receptors but no cell numbers given
Price CJ and Capogna M 2005	16033887	Neurogliaform neurons form a novel inhibitory network in the hippocampal CA1 area.	y	ratio of subtypes of NGF neurons

Price CJ and Capogna M 2008	18596171	GABA(B) receptor modulation of feedforward inhibition through hippocampal neurogliaform cells.	n	They did fill record and fill neurogliaform cells, but there is no discussion of morphological differences within the recorded population
Rapp PR and Gallagher M 1996	8790433	Preserved neuron number in the hippocampus of aged rats with spatial learning deficits.	n	
Ribak CE and Saito K 1978	75042	Immunocytochemical localization of glutamic acid decarboxylase in neuronal somata following colchicine inhibition of axonal transport.	n	describes only broad distribution of GABAergic somata, no numbers
Ribak CE and Seress L 1983	6619905	Five types of basket cell in the hippocampal dentate gyrus: a combined Golgi and electron microscopic study.	n	This paper contains a lengthy discussion of the 5 types of basket cells, and even a ratio between them, though the n is low (~ 12). However, the Hippocampome does not distinguish between the different types of basket cell (though maybe it should– they say that one doesn’t have dendrites in the hilus), so I did not take this ratio
Ribak CE and Shapiro LA 2007	17765717	Ultrastructure and synaptic connectivity of cell types in the adult rat dentate gyrus.	n	
Savic N and Sciancalepore M 2001	11353016	Electrophysiological characterization of “giant” cells in stratum radiatum of the CA3 hippocampal region.	y	There is a ratio here between CA3 radiatum giant cells that have axons in oriens and those that do not
Scharfman HE 1995	8589793	Electrophysiological diversity of pyramidal-shaped neurons at the granule cell layer/hilus border of the rat dentate gyrus recorded in vitro.	n	while 17 “pyramidal-shaped” neurons from the H/SG border region were examined, they are not clearly grouped into categories; she partitions them several times based on one or another axonal or dendritic property (which might yield many possible ratios?) but the ns are very small. Due to complexity of extraction and questionable quality, am shelving this for now.
Scharfman HE 2007	17765742	The CA3 “backprojection” to the dentate gyrus.	n	

Scharfman HE and Pierce JP 2012	22612815	New insights into the role of hilar ectopic granule cells in the dentate gyrus based on quantitative anatomic analysis and three-dimensional reconstruction.	n	review
Seress L 2007	17765710	Comparative anatomy of the hippocampal dentate gyrus in adult and developing rodents, non-human primates and humans.	n	review
Sik A and Buzsaki G 1997	9104599	Interneurons in the hippocampal dentate gyrus: an in vivo intracellular study.	n	While this contains a ratio of interneurons for the hilus (HIP, HICAP, basket), the n is extremely small– 6 neurons total
Soltész I and Deschenes M 1993	8309524	The behavior of mossy cells of the rat dentate gyrus during theta oscillations in vivo.	n	6 mossy cells were studied, but there is no description of their morphology beyond soma diameter and spininess. Therefore, due to small n and lack of detail, this cannot be used for a ratio.
Somogyi P and Klausberger T 2005	15539390	Defined types of cortical interneurone structure space and spike timing in the hippocampus.	n	review
Soriano E and Frotscher M 1989	2611653	A GABAergic axo-axonic cell in the fascia dentata controls the main excitatory hippocampal pathway.	n	They filled a bunch of cells with a Golgi stain, but were specifically looking for axo-axonic cells and they don't mention any of the others. They found 3 AA cells but only show a figure for one.
Soriano E and Frotscher M 1990	1690225	Axo-axonic chandelier cells in the rat fascia dentata: Golgi-electron microscopy and immunocytochemical studies.	n	They looked at a bunch of axo-axonic cells, but they don't talk about any other cells they filled so there are no ratios. One might think that you could get a ratio of axo-axonic in SM to axo-axonic in SG, but this actually looks like the AA they found are all in SG under our rules (they're on the very border of SM/SG)
Soriano E and Frotscher M 1993	8376624	GABAergic innervation of the rat fascia dentata: a novel type of interneuron in the granule cell layer with extensive axonal arborization in the molecular layer.	n	They have fillings of cells and nice figures, but there is no numerical breakdown and the n is unclear/very low (around 10)

Szabadics J and Soltesz I 2009	19339618	Functional specificity of mossy fiber innervation of GABAergic cells in the hippocampus.	y	ratio of interneurons in CA3
Tahyildari B and Alonso A 2005	16127693	Morphological and electrophysiological properties of lateral entorhinal cortex layers II and III principal neurons.	y	ratios for EC:II and EC:III neurons from small but reasonable sample sizes
Tort AB and Kopell NJ 2007	17679692	On the formation of gamma-coherent cell assemblies by oriens lacunosum-moleculare interneurons in the hippocampus.	n	review
Toth K and McBain CJ 1998	10196564	Afferent-specific innervation of two distinct AMPA receptor subtypes on single hippocampal interneurons.	n	They did fill and record neurons in CA3:SL, but there is no numerical breakdown of the subtypes. Also, I could not find an n for filled cells
Vida I and Frotscher M 2000	10655521	A hippocampal interneuron associated with the mossy fiber system.	y	Contains a ratio of mossy-fiber-associated to non-MFA neurons
Wenzel HJ and Schwartzkroin PA 1997	9347352	Ultrastructural localization of neurotransmitter immunoreactivity in mossy cell axons and their synaptic targets in the rat dentate gyrus.	n	mossy cells only, and there is no detailed description of full reconstructions, instead they were just looking at terminals
Williams PA and Strowbridge BW 2007	18077687	Semilunar granule cells: glutamatergic neurons in the rat dentate gyrus with axon collaterals in the inner molecular layer.	y	This contains a ratio with a big n (>200) of fast-spiking to non-fast-spiking neurons in the IML. This can be used for the ratio of SGCs to other neurons in the region, presuming all other neurons are fast spiking. Even if not, still a good constraint. Unfortunately, even though they visualized 60 neurons, only 10 of which were SGCs, they don't say anything about the other 50! Could have been a good ratio. Among the SGCs, they say only 4/10 had axons in the SMi and 3/4 of these had axons in SG. It appears there are several axo-dendritic patternings for SGCs, but the Hippocampome only records one, because no information about the SG axons was given for the 6/10 with no axon in SMi.

Williams S and LaCaille JC 1994	7931512	Membrane properties and synaptic responses of interneurons located near the stratum lacunosum-moleculare/radiatum border of area CA1 in whole-cell recordings from rat hippocampal slices.	n	while 20-some neurons were filled, they do not specify that the neurons had fully reconstructed arborizations; also, they give very little information about morphological subgroups of these interneurons; they use “sometimes” and mention specific information about 1/20 cells, so a ratio could potentially be extracted from here, but it would be weak
Witter MP 2006	16876886	Connections of the subiculum of the rat: topography in relation to columnar and laminar organization.	n	
Woodson W and Ben-Ari Y 1989	2925894	Organization of the GABAergic system in the rat hippocampal formation: a quantitative immunocytochemical study.	n	
Wouterlood FG and Witter MP 2000	10954838	Calretinin in the entorhinal cortex of the rat: distribution, morphology, ultrastructure of neurons, and co-localization with gamma-aminobutyric acid and parvalbumin.	n	they looked at some fully reconstructed CR+ neurons in the EC but I do not see a numerical breakdown anywhere of the subtypes
Zemankovics R and Hajos N 2010	20421280	Differences in subthreshold resonance of hippocampal pyramidal cells and interneurons: the role of h-current and passive membrane characteristics.	y	ratio of various CA1 interneuronal classes
Zhang W and Buckmaster PS 2009	19535596	Dysfunction of the dentate basket cell circuit in a rat model of temporal lobe epilepsy.	y	Contains a good solid ratio (many different cells) from the GC/H border region.

F.4 Abstracts Evaluated for Stereology

10196544, 10747186, 10777798, 10995835, 11067982, 11226691, 11784700, 11807843, 11920713,
12096061, 12373367, 12614688, 12625464, 14750656, 15342722, 15498801, 15927687, 16237182,
16280590, 16641241, 16930755, 17016818, 17765711, 17898215, 18077687, 18504292, 18558471,
18662340, 19020015, 19189715, 19300446, 19750211, 20130170, 20399728, 20720120, 21795545,
22161956, 22162008

F.5 Full Text Evaluated for Stereology

First/Last Authors & Year	PMID	Title	Relevant	Note
Amaral DG and Lavenex P 2007	17765709	The dentate gyrus: fundamental neuroanatomical organization (dentate gyrus for dummies).	n	review
Armstrong C and Soltesz I 2011	21452204	Neurogliaform cells in the molecular layer of the dentate gyrus as feed-forward gamma-aminobutyric acidergic modulators of entorhinal-hippocampal interplay.	n	
Ascoli GA and Barrionuevo G 2009	19496174	Quantitative morphometry of electrophysiologically identified CA3b interneurons reveals robust local geometry and distinct cell classes.	n	
Bartos M and Jonas P 2001	11306622	Rapid signaling at inhibitory synapses in a dentate gyrus interneuron network.	n	
Beed P and Schmitz D 2010	21172609	Analysis of excitatory microcircuitry in the medial entorhinal cortex reveals cell-type-specific differences.	n	
Blaabjerg M and Zimmer J 2007	17765713	The dentate mossy fibers: structural organization, development and plasticity.	n	
Blasco-Ibanez JM and Freund TF 2000	11043552	Recurrent mossy fibers preferentially innervate parvalbumin-immunoreactive interneurons in the granule cell layer of the rat dentate gyrus.	n	
Buckmaster PS and Jongen-Relo AL 1999	10531454	Highly specific neuron loss preserves lateral inhibitory circuits in the dentate gyrus of kainate-induced epileptic rats.	y	count of GAD and total neurons in DG
Bullis JB and Poolos NP 2007	17185334	Reversed somatodendritic I(h) gradient in a class of rat hippocampal neurons with pyramidal morphology.	n	

Canto CB and Witter MP 2008	18769556	What does the anatomical organization of the entorhinal cortex tell us?	n	
Cerasti E and Treves A 2010	20454678	How informative are spatial CA3 representations established by the dentate gyrus?	n	
Chevaleyre V and Siegelbaum SA 2010	20510860	Strong CA2 pyramidal neuron synapses define a powerful disynaptic cortico-hippocampal loop.	y	pyramidal cell count
Daw MI and McBain CJ 2009	19741117	Asynchronous transmitter release from cholecystokinin-containing inhibitory interneurons is widespread and target-cell independent.	n	
Dyhrfeld-Johnsen J and Soltesz I 2007	17093119	Topological determinants of epileptogenesis in large-scale structural and functional models of the dentate gyrus derived from experimental data.	n	modeling
Fuentealba P and Klausberger T 2008	18367092	Ivy cells: a population of nitric-oxide-producing, slow-spiking GABAergic neurons and their involvement in hippocampal network activity.	y	Much info on combinations of molecular markers nNOS, PV, NPY, GABA
Fuentealba P and Somogyi P 2008	18829959	Rhythmically active enkephalin-expressing GABAergic cells in the CA1 area of the hippocampus project to the subiculum and preferentially innervate interneurons.	n	
Ganter P and Somogyi P 2004	15098728	Properties of horizontal axo-axonic cells in stratum oriens of the hippocampal CA1 area of rats in vitro.	n	
Gloveli T and Buhl EH 2005	15486016	Differential involvement of oriens/pyramidal interneurons in hippocampal network oscillations in vitro.	n	
Gloveli T and Heinemann U 2001	11168548	Properties of entorhinal cortex deep layer neurons projecting to the rat dentate gyrus.	n	
Gloveli T and Kopell NJ 2005	16141320	Orthogonal arrangement of rhythm-generating microcircuits in the hippocampus.	n	

Hajos N and Freund TF 2004	15483131	Spike timing of distinct types of GABAergic interneuron during hippocampal gamma oscillations in vitro.	n	
Hamam BN and Alonso AA 2002	12209840	Morphological and electrophysiological characteristics of layer V neurons of the rat lateral entorhinal cortex.	n	
Hamam BN and Amaral DG 2000	10713573	Morphological and electrophysiological characteristics of layer V neurons of the rat medial entorhinal cortex.	n	
Harris E and Stewart M 2001	11259758	Propagation of synchronous epileptiform events from subiculum backward into area CA1 of rat brain slices.	n	
Harris E and Stewart M 2001	11406828	Intrinsic connectivity of the rat subiculum: I. Dendritic morphology and patterns of axonal arborization by pyramidal neurons.	n	
Hosseini-Sharifabad M and Nyengaard JR 2007	17368561	Design-based estimation of neuronal number and individual neuronal volume in the rat hippocampus.	y	principal cell estimates in DG, CA3, CA1
Houser CR 2007	17765721	Interneurons of the dentate gyrus: an overview of cell types, terminal fields and neurochemical identity.	n	
Jaffe DB and Gutierrez R 2007	17765714	Mossy fiber synaptic transmission: communication from the dentate gyrus to area CA3.	n	
Jinno S and Kosaka T 2010	19655319	Stereological estimation of numerical densities of glutamatergic principal neurons in the mouse hippocampus.	y	estimation of density of glutamatergic neurons in DG, CA1, CA3
Jinno S and Somogyi P 2007	17699661	Neuronal diversity in GABAergic long-range projections from the hippocampus.	n	

Karayannis T and Capogna M 2010	20660272	Slow GABA transient and receptor desensitization shape synaptic responses evoked by hippocampal neurogliaform cells.	n	
Klausberger T 2009	19735288	GABAergic interneurons targeting dendrites of pyramidal cells in the CA1 area of the hippocampus.	n	
Klausberger T and Somogyi P 2008	18599766	Neuronal diversity and temporal dynamics: the unity of hippocampal circuit operations.	n	
Larimer P and Strowbridge BW 2010	20037579	Representing information in cell assemblies: persistent activity mediated by semilunar granule cells.	n	
Lee SH and Soltesz I 2010	20534847	Distinct endocannabinoid control of GABA release at perisomatic and dendritic synapses in the hippocampus.	n	
Leranth C and Hajszan T 2007	17765712	Extrinsic afferent systems to the dentate gyrus.	n	
Losonczy A and Nusser Z 2004	14734812	Persistently active cannabinoid receptors mute a subpopulation of hippocampal interneurons.	n	
Mercer A and Thomson AM 2007	17611285	Characterization of neurons in the CA2 subfield of the adult rat hippocampus.	n	
Mercer A and Thomson AM 2012	20882544	Local circuitry involving parvalbumin-positive basket cells in the CA2 region of the hippocampus.	n	
Miettinen R and Leranth C 2012	22230770	Estimation of the total number of hippocampal CA1 pyramidal neurons: new methodology applied to helpless rats.	n	no markers, only total CA1:SP neuron count
Miki T and Takeuchi Y 2005	16158978	Application of the physical disector to the central nervous system: estimation of the total number of neurons in subdivisions of the rat hippocampus.	y	counts of principal cells and hilar neurons CA1 CA3 DG

- Morgan RJ and Soltesz I 2007 17765743 Modeling the dentate gyrus. n
- Naber PA and Witter MP 2001 11345131 Reciprocal connections between the entorhinal cortex and hippocampal fields CA1 and the subiculum are in register with the projections from CA1 to the subiculum. n
- O'Mara SM and Gigg J 2001 11240210 The subiculum: a review of form, physiology and function. n review
- Poolos NP and Roth MK 2006 16870744 Modulation of h-channels in hippocampal pyramidal neurons by p38 mitogen-activated protein kinase. n
- Price CJ and Capogna M 2005 16033887 Neurogliaform neurons form a novel inhibitory network in the hippocampal CA1 area. n
- Price CJ and Capogna M 2008 18596171 GABA(B) receptor modulation of feedforward inhibition through hippocampal neurogliaform cells. n
- Ribak CE and Shapiro LA 2007 17765717 Ultrastructure and synaptic connectivity of cell types in the adult rat dentate gyrus. n
- Savic N and Sciancalepore M 2001 11353016 Electrophysiological characterization of "giant" cells in stratum radiatum of the CA3 hippocampal region. n
- Scharfman HE 2007 17765742 The CA3 "backprojection" to the dentate gyrus. n
- Seress L 2007 17765710 Comparative anatomy of the hippocampal dentate gyrus in adult and developing rodents, non-human primates and humans. n review
- Somogyi P and Klausberger T 2005 15539390 Defined types of cortical interneurone structure space and spike timing in the hippocampus. n
- Szabadics J and Soltesz I 2009 19339618 Functional specificity of mossy fiber innervation of GABAergic cells in the hippocampus. n

Szabadics J and Soltesz I 2010	20554881	Granule cells in the CA3 area.	y	stereology of Prox1 and CB used to identify CA3 granule cell population
Tahyildari B and Alonso A 2005	16127693	Morphological and electrophysiological properties of lateral entorhinal cortex layers II and III principal neurons.	n	
Tort AB and Kopell NJ 2007	17679692	On the formation of gamma-coherent cell assemblies by oriens lacunosum-moleculare interneurons in the hippocampus.	n	review
Toth K and McBain CJ 1998	10196564	Afferent-specific innervation of two distinct AMPA receptor subtypes on single hippocampal interneurons.	n	
Vida I and Frotscher M 2000	10655521	A hippocampal interneuron associated with the mossy fiber system.	n	
Witter MP 2006	16876886	Connections of the subiculum of the rat: topography in relation to columnar and laminar organization.	n	
Wouterlood FG and Witter MP 2000	10954838	Calretinin in the entorhinal cortex of the rat: distribution, morphology, ultrastructure of neurons, and co-localization with gamma-aminobutyric acid and parvalbumin.	y	CR and GABA relationship in the EC
Zemankovics R and Hajos N 2010	20421280	Differences in subthreshold resonance of hippocampal pyramidal cells and interneurons: the role of h-current and passive membrane characteristics.	n	

Bibliography

Bibliography

- [1] D G Amaral. A Golgi study of cell types in the hilar region of the hippocampus in the rat. *The Journal of comparative neurology*, 182(4 Pt 2):851–914, December 1978.
- [2] David G Amaral, Norio Ishizuka, and Brenda Claiborne. Chapter neurons, numbers and the hippocampal network. *Progress in brain research*, 83:1–11, 1990.
- [3] DG Amaral and P. Lavenex. Hippocampal neuroanatomy. *The Hippocampus Book*, 1(3):37–114, 2007.
- [4] Caren Armstrong, János Szabadics, Gabor Tamas, and Ivan Soltesz. Neurogliaform cells in the molecular layer of the dentate gyrus as feed-forward γ -aminobutyric acidergic modulators of entorhinal-hippocampal interplay. *The Journal of comparative neurology*, 519(8):1476–1491, June 2011.
- [5] T L Babb, J K Pretorius, W R Kupfer, and W J Brown. Distribution of glutamate-decarboxylase-immunoreactive neurons and synapses in the rat and monkey hippocampus: light and electron microscopy. *The Journal of comparative neurology*, 278(1):121–138, December 1988.
- [6] M. Bartos, J.F. Sauer, I. Vida, and Á. Kulik. Fast and Slow GABAergic Transmission in Hippocampal Circuits. *Hippocampal Microcircuits*, pages 129–161, 2010.
- [7] M. Bartos, I. Vida, M Frotscher, J R Geiger, and P Jonas. Rapid signaling at inhibitory synapses in a dentate gyrus interneuron network. *Journal of Neuroscience*, 21(8):2687–2698, April 2001.
- [8] Marianne J Bezaire and Ivan Soltesz. Quantitative assessment of CA1 local circuits: Knowledge base for interneuron-pyramidal cell connectivity. *Hippocampus*, May 2013.
- [9] B D Boss, G M Peterson, and W M Cowan. On the number of neurons in the dentate gyrus of the rat. *Brain research*, 338(1):144–150, July 1985.
- [10] P S Buckmaster and A L Jongen-Rêlo. Highly specific neuron loss preserves lateral inhibitory circuits in the dentate gyrus of kainate-induced epileptic rats. *Journal of Neuroscience*, 19(21):9519–9529, November 1999.
- [11] P S Buckmaster, B W Strowbridge, D D Kunkel, D L Schmiede, and P A Schwartzkroin. Mossy cell axonal projections to the dentate gyrus molecular layer in the rat hippocampal slice. *Hippocampus*, 2(4):349–362, October 1992.

- [12] Paul S Buckmaster. Mossy cell dendritic structure quantified and compared with other hippocampal neurons labeled in rats in vivo. *Epilepsia*, 53 Suppl 1:9–17, June 2012.
- [13] K Ceranik, R Bender, J R Geiger, H Monyer, P Jonas, M Frotscher, and J Lübke. A novel type of GABAergic interneuron connecting the input and the output regions of the hippocampus. *The Journal of neuroscience : the official journal of the Society for Neuroscience*, 17(14):5380–5394, July 1997.
- [14] Jonas Dyhrfeld-Johnsen, Vijayalakshmi Santhakumar, Robert J Morgan, Ramon Huerta, Lev Tsimring, and Ivan Soltesz. Topological determinants of epileptogenesis in large-scale structural and functional models of the dentate gyrus derived from experimental data. *Journal of neurophysiology*, 97(2):1566–1587, February 2007.
- [15] Tamas F Freund and G Buzsaki. Interneurons of the hippocampus. *Hippocampus*, 6(4):347–470, 1996.
- [16] F B Gaarskjaer. Organization of the mossy fiber system of the rat studied in extended hippocampi. I. Terminal area related to number of granule and pyramidal cells. *The Journal of comparative neurology*, 178(1):49–72, March 1978.
- [17] A I Gulyás, N Hájos, and Tamas F Freund. Interneurons containing calretinin are specialized to control other interneurons in the rat hippocampus. *The Journal of neuroscience : the official journal of the Society for Neuroscience*, 16(10):3397–3411, May 1996.
- [18] N Hájos, L Acsády, and Tamas F Freund. Target selectivity and neurochemical characteristics of VIP-immunoreactive interneurons in the rat dentate gyrus. *European Journal of Neuroscience*, 8(7):1415–1431, July 1996.
- [19] Z S Han. Electrophysiological and morphological differentiation of chandelier and basket cells in the rat hippocampal formation: a study combining intracellular recording and intracellular staining with biocytin. *Neuroscience research*, 19(1):101–110, February 1994.
- [20] Z S Han, E H Buhl, Z Lörinczi, and P Somogyi. A high degree of spatial selectivity in the axonal and dendritic domains of physiologically identified local-circuit neurons in the dentate gyrus of the rat hippocampus. *European Journal of Neuroscience*, 5(5):395–410, May 1993.
- [21] K Horikawa and W E Armstrong. A versatile means of intracellular labeling: injection of biocytin and its detection with avidin conjugates. *Journal of Neuroscience Methods*, 25(1):1–11, August 1988.
- [22] Mohammad Hosseini-Sharifabad and Jens Randel Nyengaard. Design-based estimation of neuronal number and individual neuronal volume in the rat hippocampus. *Journal of Neuroscience Methods*, 162(1-2):206–214, May 2007.
- [23] Carolyn R Houser. Interneurons of the dentate gyrus: an overview of cell types, terminal fields and neurochemical identity. *Progress in brain research*, 163:217–232, 2007.

- [24] Yiqun Jiao and J Victor Nadler. Stereological analysis of GluR2-immunoreactive hilar neurons in the pilocarpine model of temporal lobe epilepsy: correlation of cell loss with mossy fiber sprouting. *Experimental neurology*, 205(2):569–582, June 2007.
- [25] Shozo Jinno and Toshio Kosaka. Cellular architecture of the mouse hippocampus: a quantitative aspect of chemically defined GABAergic neurons with stereology. *Neuroscience research*, 56(3):229–245, November 2006.
- [26] I Katona, L Acsády, and Tamas F Freund. Postsynaptic targets of somatostatin-immunoreactive interneurons in the rat hippocampus. *Neuroscience*, 88(1):37–55, January 1999.
- [27] C Köhler and V Chan-Palay. Somatostatin-like immunoreactive neurons in the hippocampus: an immunocytochemical study in the rat. *Neuroscience letters*, 34(3):259–264, December 1982.
- [28] Phillip Larimer and Ben W Strowbridge. Representing information in cell assemblies: persistent activity mediated by semilunar granule cells. *Nature neuroscience*, 13(2):213–222, February 2010.
- [29] X G Li, P Somogyi, J M Tepper, and G Buzsáki. Axonal and dendritic arborization of an intracellularly labeled chandelier cell in the CA1 region of rat hippocampus. *Experimental brain research. Experimentelle Hirnforschung. Expérimentation cérébrale*, 90(3):519–525, 1992.
- [30] J Lübke, M Frotscher, and N. Spruston. Specialized electrophysiological properties of anatomically identified neurons in the hilar region of the rat fascia dentata. *Journal of neurophysiology*, 79(3):1518–1534, March 1998.
- [31] Sean J Markwardt, Cristina V Dieni, Jacques I Wadiche, and Linda Overstreet-Wadiche. Ivy/neurogliaform interneurons coordinate activity in the neurogenic niche. *Nature neuroscience*, 14(11):1407–1409, November 2011.
- [32] A Martí-Subirana, E Soriano, and J M García-Verdugo. Morphological aspects of the ectopic granule-like cellular populations in the albino rat hippocampal formation: a Golgi study. *Journal of anatomy*, 144:31–47, February 1986.
- [33] Daniel P McCloskey, Tana M Hintz, Joseph P Pierce, and Helen E Scharfman. Stereological methods reveal the robust size and stability of ectopic hilar granule cells after pilocarpine-induced status epilepticus in the adult rat. *European Journal of Neuroscience*, 24(8):2203–2210, October 2006.
- [34] Takanori Miki, Irawan Satriotomo, Hong-Peng Li, Yoshiki Matsumoto, He Gu, Toshifumi Yokoyama, Kyoung-Youl Lee, Kuldip S Bedi, and Yoshiki Takeuchi. Application of the physical disector to the central nervous system: estimation of the total number of neurons in subdivisions of the rat hippocampus. *Anatomical science international*, 80(3):153–162, September 2005.
- [35] R.J. Morgan and I Soltesz. Microcircuit Model of the Dentate Gyrus in Epilepsy. *Hippocampal Microcircuits*, pages 495–525, 2010.

- [36] Robert J Morgan, Vijayalakshmi Santhakumar, and Ivan Soltesz. Modeling the dentate gyrus. *Progress in brain research*, 163:639–658, 2007.
- [37] D D Mott, Q Li, M M Okazaki, D A Turner, and D V Lewis. GABAB-Receptor-mediated currents in interneurons of the dentate-hilus border. *Journal of neurophysiology*, 82(3):1438–1450, September 1999.
- [38] D D Mott, D A Turner, M M Okazaki, and D V Lewis. Interneurons of the dentate-hilus border of the rat dentate gyrus: morphological and electrophysiological heterogeneity. *The Journal of neuroscience : the official journal of the Society for Neuroscience*, 17(11):3990–4005, June 1997.
- [39] T Nomura, T Fukuda, Y Aika, C W Heizmann, P C Emson, T Kobayashi, and T Kosaka. Distribution of nonprincipal neurons in the rat hippocampus, with special reference to their dorsoventral difference. *Brain research*, 751(1):64–80, March 1997.
- [40] T Nomura, T Fukuda, Y Aika, C W Heizmann, P C Emson, T Kobayashi, and T Kosaka. Laminar distribution of non-principal neurons in the rat hippocampus, with special reference to their compositional difference among layers. *Brain research*, 764(1-2):197–204, August 1997.
- [41] P E Patton and B McNaughton. Connection matrix of the hippocampal formation: I. The dentate gyrus. *Hippocampus*, 5(4):245–286, 1995.
- [42] S J Pleasure, A E Collins, and D H Lowenstein. Unique expression patterns of cell fate molecules delineate sequential stages of dentate gyrus development. *The Journal of neuroscience : the official journal of the Society for Neuroscience*, 20(16):6095–6105, August 2000.
- [43] P R Rapp and M Gallagher. Preserved neuron number in the hippocampus of aged rats with spatial learning deficits. *Proceedings of the National Academy of Sciences of the United States of America*, 93(18):9926–9930, September 1996.
- [44] C E Ribak, R Nitsch, and L Seress. Proportion of parvalbumin-positive basket cells in the GABAergic innervation of pyramidal and granule cells of the rat hippocampal formation. *The Journal of comparative neurology*, 300(4):449–461, October 1990.
- [45] C E Ribak and L Seress. Five types of basket cell in the hippocampal dentate gyrus: a combined Golgi and electron microscopic study. *Journal of neurocytology*, 12(4):577–597, August 1983.
- [46] V. Santhakumar. Modeling Circuit Alterations in Epilepsy: A Focus on Mossy Cell Loss and Mossy Fiber Sprouting in the Dentate Gyrus. *Computational neuroscience in epilepsy*, page 89, 2008.
- [47] Vijayalakshmi Santhakumar, Ildiko Aradi, and Ivan Soltesz. Role of mossy fiber sprouting and mossy cell loss in hyperexcitability: a network model of the dentate gyrus incorporating cell types and axonal topography. *Journal of neurophysiology*, 93(1):437–453, January 2005.

- [48] H E Scharfman. Electrophysiological diversity of pyramidal-shaped neurons at the granule cell layer/hilus border of the rat dentate gyrus recorded in vitro. *Hippocampus*, 5(4):287–305, 1995.
- [49] Helen E Scharfman and Catherine E Myers. Hilar mossy cells of the dentate gyrus: a historical perspective. *Frontiers in neural circuits*, 6:106, 2012.
- [50] Helen E Scharfman and Joseph P Pierce. New insights into the role of hilar ectopic granule cells in the dentate gyrus based on quantitative anatomic analysis and three-dimensional reconstruction. *Epilepsia*, 53 Suppl 1:109–115, June 2012.
- [51] A R Schlessinger, W M Cowan, and D I Gottlieb. An autoradiographic study of the time of origin and the pattern of granule cell migration in the dentate gyrus of the rat. *The Journal of comparative neurology*, 159(2):149–175, January 1975.
- [52] L Seress and J Pokorny. Structure of the granular layer of the rat dentate gyrus. A light microscopic and Golgi study. *Journal of anatomy*, 133(Pt 2):181–195, September 1981.
- [53] R S Sloviter, L Ali-Akbarian, K D Horvath, and K A Menkens. Substance P receptor expression by inhibitory interneurons of the rat hippocampus: enhanced detection using improved immunocytochemical methods for the preservation and colocalization of GABA and other neuronal markers. *The Journal of comparative neurology*, 430(3):283–305, February 2001.
- [54] I Soltesz, J Bourassa, and M Deschênes. The behavior of mossy cells of the rat dentate gyrus during theta oscillations in vivo. *Neuroscience*, 57(3):555–564, December 1993.
- [55] E Soriano and M Frotscher. A GABAergic axo-axonic cell in the fascia dentata controls the main excitatory hippocampal pathway. *Brain research*, 503(1):170–174, November 1989.
- [56] E Soriano and M Frotscher. GABAergic innervation of the rat fascia dentata: a novel type of interneuron in the granule cell layer with extensive axonal arborization in the molecular layer. *The Journal of comparative neurology*, 334(3):385–396, August 1993.
- [57] E Soriano and M Frotscher. Mossy cells of the rat fascia dentata are glutamate-immunoreactive. *Hippocampus*, 4(1):65–69, February 1994.
- [58] János Szabadics, Csaba Varga, János Brunner, Kang Chen, and Ivan Soltesz. Granule cells in the CA3 area. *Journal of Neuroscience*, 30(24):8296–8307, June 2010.
- [59] N M van Strien, N L M Cappaert, and M.P. Witter. The anatomy of memory: an interactive overview of the parahippocampal-hippocampal network. *Nature reviews. Neuroscience*, 10(4):272–282, April 2009.
- [60] M J West. Stereological methods for estimating the total number of neurons and synapses: issues of precision and bias. *Trends in neurosciences*, 22(2):51–61, 1999.
- [61] M J West and A H Andersen. An allometric study of the area dentata in the rat and mouse. *Brain research*, 2(3):317–348, December 1980.

- [62] M J West, P D Coleman, and D G Flood. Estimating the number of granule cells in the dentate gyrus with the disector. *Brain research*, 448(1):167–172, May 1988.
- [63] MJ West, L Slomianka, and H J G Gundersen. Unbiased stereological estimation of the total number of neurons in the subdivisions of the rat hippocampus using the optical fractionator. *The Anatomical Record*, 231(4):482–497, 1991.
- [64] Philip A Williams, Phillip Larimer, Yuan Gao, and Ben W Strowbridge. Semilunar granule cells: glutamatergic neurons in the rat dentate gyrus with axon collaterals in the inner molecular layer. *Journal of Neuroscience*, 27(50):13756–13761, December 2007.
- [65] W Woodson, L Nitecka, and Y Ben-Ari. Organization of the GABAergic system in the rat hippocampal formation: a quantitative immunocytochemical study. *The Journal of comparative neurology*, 280(2):254–271, February 1989.
- [66] Yang Xiang, Sylvain Gubian, Brian Suomela, and Julia Hoeng. Generalized simulated annealing for global optimization: the gensa package.
- [67] Wei Zhang and Paul S Buckmaster. Dysfunction of the dentate basket cell circuit in a rat model of temporal lobe epilepsy. *Journal of Neuroscience*, 29(24):7846–7856, June 2009.

Curriculum Vitae

Sean Mackesey was born in Fairfax, Virginia in 1986. He received his BA in chemistry from Northwestern University in 2008. He has worked as a lifeguard, a canvasser, an English teacher, and a tutor.